Naval Research Laboratory
Stennis Space Center, MS 39529-5004

NRL/FR/7320--02-10,035

The U.S. Navy's Global Wind-Wave Models: An Investigation into Sources of Errors in Low-Frequency Energy Predictions

W. ERICK ROGERS

Ocean Dynamics and Prediction Branch
Oceanography Division

October 18, 2002

REPORT DOCUMENTATION PAGE

Form Approved
OMB No. 0704-0188

1. REPORT DATE *(DD-MM-YYYY)*	2. REPORT TYPE	3. DATES COVERED *(From - To)*
October 18, 2002	Interim	

4. TITLE AND SUBTITLE

The U.S. Navy's Global Wind-Wave Models: An Investigation into Sources of Error in Low-Frequency Energy Predictions

5a. CONTRACT NUMBER

5b. GRANT NUMBER

5c. PROGRAM ELEMENT NUMBER

6. AUTHOR(S)

W. Erick Rogers

5d. PROJECT NUMBER

5e. TASK NUMBER

5f. WORK UNIT NUMBER

7. PERFORMING ORGANIZATION NAME(S) AND ADDRESS(ES)

Naval Research Laboratory
Oceanography Division
Stennis Space Center, MS 39529-5004

8. PERFORMING ORGANIZATION REPORT NUMBER

NRL/FR/7320--02-10,035

9. SPONSORING / MONITORING AGENCY NAME(S) AND ADDRESS(ES)

Office of Naval Research
800 North Quincy Street
Arlington, VA 22217-5660

10. SPONSOR / MONITOR'S ACRONYM(S)

ONR

11. SPONSOR / MONITOR'S REPORT NUMBER(S)

12. DISTRIBUTION / AVAILABILITY STATEMENT

Approved for public release; distribution is unlimited.

13. SUPPLEMENTARY NOTES

14. ABSTRACT

This report describes an investigation to determine the relative importance of various sources of error in the two global-scale models of wind-generated surface waves used operationally by the U.S. Navy. The investigation is limited to low-frequency wave energy (e.g., less than 0.08 Hz). Sources of error are grouped into three broad categories: (1) wave model propagation numerics and resolution, (2) wave model physical formulations, and (3) wind forcing (provided to the wave model by an atmospheric model and/or data assimilation system). Each of the three is described and studied independently using tests and hindcasts of varying complexity. Based on these studies, it appears that in both of the Navy models, numerics and resolution are not first-order sourcess of error, and further suggests that, at present, more error is due to model forcing than due to physical formulation. The importance of accuately capturing the intensity of high-speed wind events is shown to be paramount. Also, it appears that the practical effect of physical formulations on swell in the two operational models is considerably different, whereas differences associated with the generation (low-frequency wave growth) stage are relatively modest between the two models.

15. SUBJECT TERMS

Swell; WAM; WAVEWATCH-III, NOGAPS, QuikSCAT; Scatterometer; Wind-waves; Gravity-waves; Surf; NDBC; Buoy; Surface winds

16. SECURITY CLASSIFICATION OF:			17. LIMITATION OF ABSTRACT	18. NUMBER OF PAGES	19a. NAME OF RESPONSIBLE PERSON
a. REPORT	b. ABSTRACT	c. THIS PAGE			Erick Rogers
Unclassified	Unclassified	Unclassified	UL	67	19b. TELEPHONE NUMBER *(include area code)* (228) 688-4727

Standard Form 298 (Rev. 8-98)
Prescribed by ANSI Std. Z39.18

CONTENTS

EXECUTIVE SUMMARY

This report describes an investigation to determine the relative importance of various sources of error in the two global-scale wave models used operationally by the U.S. Navy. The investigation is limited to low-frequency wave energy (e.g., less than 0.08 Hz). Sources of error are grouped into three broad categories: (1) wave model numerics and resolution, (2) wave model physical formulations, and (3) wind forcing (provided to the wave model by an atmospheric model and/or data assimilation system). First, each of the three is described and studied independently using relatively simple tests and comparisons. Based on these studies, it appears that in both of the Navy models, numerics and resolution are not a first-order source of error; physics and wind forcing both appear to be important, although their relative importance is not yet determined. The investigation is continued by applying the Navy's wave models to three global hindcasts, each of approximately 1-month duration. The hindcasts are applied with two different propagation numerics techniques, three different physical formulations, and three different forcing techniques. The three sources of error are each studied in turn by varying one while holding the other two constant in the hindcasts. This analysis confirms that propagation numerics are not a first-order source of error in the Navy models, and further suggests that, at present, more error is due to model forcing than to physical formulation.

One of the three forcing techniques is a method developed as part of this study: a simplistic method of blending satellite scatterometer data with atmospheric model output. The results were favorable. Several (still relatively simple) ways remain in which this technique can be improved. This suggests that the technique has great potential for creating wind fields for forcing global wave model hindcasts. But more importantly, these wind fields could potentially be created operationally to dramatically reduce negative biases in Navy swell forecasts.

THE U.S. NAVY'S GLOBAL WIND-WAVE MODELS: AN INVESTIGATION INTO SOURCES OF ERROR IN LOW-FRQUENCY ENERGY PREDICTIONS

1. INTRODUCTION

Motivation and Objective

The ultimate goal associated with this investigation–in broad terms–is to enable the operational Navy to produce more accurate forecasts of wind-generated waves. The primary specific motivation is to improve surf forecasts (important for naval operations in the nearshore), with the secondary goal being better forecasts of the general global wave climate (e.g., for ship operational safety).

A smaller scale wave model (e.g., regional-scale model or surf model), which relies on a global model for boundary forcing (either directly or indirectly), will obviously have little chance of success if the global model is not accurate. It is already known that the Navy's global models are often inaccurate, but it is much more difficult to determine conclusively the cause of the error in the global models (see, e.g., Wittmann and O'Reilly 1998). The latter is the objective of this study.

The source/sink terms used in today's models cannot yet be tuned in a "universal" manner, equally applicable at smaller and larger scale (see, e.g., Tolman 2002a). This leads to a situation where a global model must be tuned using global (or near-global) scale simulations, as opposed to, for example, short-fetch growth curves. Thus the model must be tuned in situations where other sources of error (besides source/sink terms) are present. Intimate familiarity with impact of various sources of error in the models should therefore be a prerequisite for model development.

In terms of forecasting ability, swell is particularly important, simply because of the inherent difficulty in forecasting these waves. When surf is badly underpredicted, it is often a case of "missing swell." Swell presents the greatest potential "surprise factor" with regard to wave forecasts. With a reasonably accurate meteorological forecast, a sailor will generally not be surprised by rough wind seas. Swell, on the other hand requires a greater level of sophistication to forecast, e.g., a numerical model.

Low-Frequency Energy

As the title implies, we limit our focus to low-frequency wave energy (e.g., 0.08 Hz and lower). This is for several reasons. First of all, swell (important for reasons discussed above) is primarily of low frequency. Secondly, low-frequency waves shoal more dramatically than higher frequency waves, making them disproportionately important to nearshore operations. Longer waves can become higher than shorter waves (due to geometric limitation on steepness), and thus potentially more problematic to naval operations when they break.

Manuscript approved July 30, 2002.

Also, by studying only the lower frequency region of the wave spectrum, we limit the scope of our problem somewhat (making it more manageable), and remove much of the clutter of the problem (namely, the short waves that are ubiquitous on the ocean's surface). This allows us to better visualize the trends in the remaining spectrum.

There are, of course, drawbacks to this approach. Most importantly, altimeter wave heights provide only the total wave height (based on all frequency components), so we cannot use altimetry to quantify low-frequency energy. Altimetry is otherwise an excellent means of validating a global model, since it is measured globally, whereas in situ data are not (e.g., buoys are particularly sparse in the Southern Hemisphere). Furthermore, there is a danger that improving predictions of low frequency energy will degrade predictions of total energy. This is very important since total wave height is the most common measure of model skill in the operational Navy. For example, if energy predictions are biased high in the high frequencies, and if we improve our model by reducing a negative bias in low-frequency prediction, we could be introducing a positive bias in total wave height where it did not already exist.

Low-frequency Wave Height Definition

In most of our comparisons between models and buoy data, we use the quantity "low frequency wave height." This is calculated from the variance (energy) of the wave spectrum below some specific frequency:

$$H_{m0,L} = 4\sqrt{\upsilon_L} \text{ and } \upsilon_L = \int_{f_1}^{f_L} E(f)df,$$

where υ_L is the "low-frequency variance," E is spectral density, f is frequency, f_1 is the lowest represented frequency in the model or data, and subscript L denotes the highest frequency included in the calculation (we generally used 0.06, 0.08, and/or 0.10Hz in our comparisons). The lower bound of the integration is (strictly speaking) not the lowest specified frequency (say, "f_{s1}") but something slightly lower. In the context of a model with a logarithmic frequency distribution, $f_1 = f_{s1} - \Delta f_{s1}$ might be used. In the context of buoy data with uniform frequency distribution, it is exactly $f_1 = f_{s1} - \Delta f_{s1}$. We use this stricter definition. Note however, that the lowest described frequency typically has very small spectral density, so this is probably a case of being correct for aesthetic reasons. Spectra are assumed continuous in frequency space, with linear variation of E between the frequencies at which E is specified in model or data. The integration is then calculated exactly (by trapezoidal method), with interpolation such that the integration stops at f_L in both model and data. We note that in the context of buoy data in which frequency bins are of uniform width, there is a simpler method of calculating variance. Where Δf is the bandwidth, variance can simply be calculated as

$$\upsilon_L = \sum_{f_1}^{f_L} E(f)\Delta f.$$

This is mathematically identical to the interpolation/integration method, provided the bandwidths of the first and last frequencies are correctly specified in both cases.

This low-frequency metric has certain advantages:

- A "wave height," unlike spectral density for example, is something readily understood.
- The integration has the advantage of removing much of the uncertainty (high confidence limits) associated with energy density derived from buoy measurements.

But there are also disadvantages:

- It is not a "real" wave height, insofar as it is not representative of the entire spectrum. It is the wave height that would be calculated if the higher frequency components did not exist.
- If $H_{m0,L}$ is calculated for multiple values of f_L, there is a certain amount of redundancy, insofar as the lowest frequencies (e.g., 0.05 Hz) are included in all of the $H_{m0,L}$ calculations.

There are alternative methods. For example, time series of variance density at several frequencies might be presented (Rogers et al. 2002a), but with a moving average in time (e.g., a 3-h average of $E(f)$) to reduce problems with data confidence limits. Or, a moving average in frequency space might be used. For example, the spectrally local variance might be calculated as

$$v_f = \int_{f-\Delta f_c}^{f+\Delta f_c} E(f)df,$$

where Δf_c is some frequency interval coarser than that of model or data (e.g., integration bounds of $f \pm 0.02$ Hz).

QuikSCAT Scatterometry

At several points in this report, we make use of QuikSCAT data. This refers to wind information derived from scatterometer data collected by the SeaWinds instrument on the QuikSCAT satellite. At present (June 2002), QuikSCAT data are the only scatterometer data being collected (ERS-2 is still operating, but is no longer providing scatterometer data). For more information on scatterometer data, see Schlax et al. (2001), Atlas et al. (2001), Dickenson et al. (2001), Freilich and Dunbar (1999), Portabella and Stoffelen (2001), and references therein. QuikSCAT was launched in June 1999. This mission has a significant advantage over all other scatterometer missions because of its broad swath: every 24 hours, the SeaWinds instrument measures approximately 90% of the non-ice ocean. Wind speed information is also provided by altimeter (e.g., TOPEX), but it is now generally believed that altimeter-derived wind speeds are of significantly lower quality than those derived from scatterometry.

We obtain our QuikSCAT data from the Jet Propulsion Laboratory (JPL). (This is provided (free of charge, via anonymous ftp) by the Physical Oceanography Distributed Active Archive Center of JPL. The data and documents describing the data are found at http://podaac.jpl.nasa.gov/quikscat/.) We use the data provided in two forms: Level 2B (L2B) and Level 3 (L3). Both data sets provide wind vectors and retain temporal information associated with the time of measurement. The L2B data are given in 25-km^2 cells. The swaths are 72-76 cells across. The L3 data are given on a regular 0.25° grid (which is similar to the L2B resolution), with the data separated into ascending and descending passes. The L2B data contain more information than L3 (e.g., regarding data quality, direction ambiguities, etc.). The L3 data contain numerous empty grid cells, presumably where data quality was deemed too poor. Thus, L3 can be considered a more "processed" product, while L2B is a product in which more is left to the judgment of the end user. PODAAC (2001a, 2001b) provide further descriptions of these products.

2. THE NAVY'S OPERATIONAL GLOBAL WAVE MODELS

General Description

At the present time (July 2002), two wave models are being run operationally at global scale by the Navy: WAM Cycle 4 (WAM4) at the Naval Oceanographic Office (NAVO) (WAMDI Group 1988, Günther et al. 1992, Komen et al. 1994), and WAVEWATCH III (WvW3) at the Fleet Numerical Meteorology and Oceanography Center (FNMOC) (Tolman 1991, Tolman and Chalikov 1996, Tolman 1999). Both are known as third-generation wave models. Recent reviews of the Navy's operational global wave models are found in Jensen et al. (2002) and Wittmann (2001). Two earlier references are Wittmann and Clancy (1993) and Wittmann et al. (1995).

Both models are phase-averaged and stochastic. This implies that output from the model is relevant on time scales longer than the waves themselves, and that computational geographic resolution can be much greater than one wavelength.

Governing Equations

The governing equation of WAM4 is the energy balance equation,

$$\frac{\partial}{\partial t} E + (\cos\varphi)^{-1} \frac{\partial}{\partial \varphi} \dot{\varphi} \cos\varphi \, E + \frac{\partial}{\partial \lambda} \dot{\lambda} E + \frac{\partial}{\partial \theta} \dot{\theta} E = S, \tag{1}$$

where t is time, λ is longitude, φ is latitude, q is wave direction, and E is the wave energy density spectrum, described in five dimensions (φ, λ, f, q, t), The $\bullet$ symbol denotes the wave action propagation speed in (φ, λ, f, q) space, f is the frequency, and S is the total of source/sink terms. The source/sink terms are often referred to as the "physics" of a wave model. The governing equation for WvW3 is the action balance equation. Wave action density is equal to energy density divided by relative frequency ($N = E/s$). If currents are not considered–which is presently the case at NAVO, FNMOC, and the National Center for Environmental Prediction (NCEP)–then these two governing equations are essentially identical. See WAMDI Group (1988) for more detail on the energy balance equation and the formulation of WAM; see Komen et al. (1994), Section III.2 for more detail regarding the action balance equation and changes associated with WAM Cycle 4; and see Tolman (1999) for more detail regarding WvW3. Other significant differences exist between the design of WAM4 and WvW3. For example, WvW3 is solved in wavenumber space, rather than in frequency space.

Physical Formulations

In deep water, S is dominated by three terms, $S \approx S_{in} + S_{nl} + S_{d}$: input by wind (which can be negative in the case of WvW3), four-wave nonlinear interactions, and dissipation, respectively. The physics of WAM4 are described in Komen et al. (1994); the physics of WvW3 are described in Tolman and Chalikov (1996), with minor refinement of the Tolman and Chalikov physics being described in Tolman (1999). The WvW3 formulations of S_{in} and S_{ds} are quite different from those of WAM4. With regard to the S_{nl}, there is only a minor difference. The S formulation of Tolman (1999) is henceforth denoted TC (Tolman and Chalikov) physics. For the most part, the physical formulations of these two models are based on earlier works, some of which are not referenced here.

Numerical Formulations

Both WAM4 and WvW3 use finite differencing methods to approximate the partial differential equation (PDE) given in Eq. (1). WAM4 uses first-order approximations (the first-order, upwind, explicit scheme; see WAMDI Group 1988). WvW3 includes (as an option) the same first-order scheme as WAM, but by default it uses higher order approximations, namely the QUICKEST scheme of Leonard (1979) and Davis and Moore (1982), combined with the ULTIMATE total variance diminishing limiter (Leonard, 1991). See Tolman (1995) for more information. WvW3 uses a dynamically adjusted source term time step (Tolman 1992).

3. CATEGORIZATION OF ERROR

We group sources of error in the Navy's operational global wave models (WAM and WvW3) into three broad categories: numerics and resolution, physics, and forcing.

Numerics and Resolution (Propagation)

There are essentially two stages of wave modeling: generation and propagation. During propagation, errors due to the numerics and resolution used in a model accumulate. This is relevant to propagation in both geographic space and spectral space (e.g., propagation between directional bins due to great circle turning).

Propagation Numerics

The truncation error associated with finite-difference approximations of the PDE (Eq. (1)) manifest as numerical diffusion and dispersion in the model solution. As swell is propagated across large distances, numerical errors in the swell field can become quite significant. Obviously, this error (diffusion in particular) is more severe in the WAM model (compared to WvW3) due to the first-order accuracy of the WAM finite-differencing scheme.

Numerical diffusion has the effect of smoothing features in a wave field as it propagates. This tends to reduce maxima (either in the geographic distribution of wave energy, or in time series at a particular geographic location) and increase minima.

One effect of numerical dispersion is to alter the apparent propagation speed of a feature in the wave field. For example, a given spectral component may arrive at a location slightly late or early. Dispersion also leads to "wiggles:" aphysical features in the wave field that appear because different Fourier components of the numerical solution travel with different numerical phase speeds. Wiggles tend to be more problematic with higher order schemes, since the diffusion of first-order schemes tends to mask the numerical dispersion.

Diffusion and dispersion are mass-conserving processes: positive error at one time/location tends to be accompanied by negative error somewhere else. At a given geographic location, some spectral components may have significant errors associated with geographic propagation numerics, while another spectral component may have much smaller error, or error of opposite sign. Thus, the effect of numerical geographic propagation error on wave height (the integrated wave spectrum) tends to be smaller than its effect on individual spectral components (of swell). Similarly, in animations of global distributions of wave heights, it is often difficult to distinguish *real* dispersion from *artificial* diffusion (both will spread energy geographically during propagation) without also looking at individual components of the wave spectra.

In the literature, numerical diffusion in wave models is sometimes discussed using terms such as "attenuation" and "dissipation" (e.g., Bender 1996). In the context of gravity waves, these terms imply a loss of energy. Based on this, a consistent negative bias in wave energy could be attributed to the inaccuracy of a first-order propagation scheme. However, diffusion associated with the numerical schemes of these models is mass-conserving. Thus "attenuation" and "dissipation" are correct terminology if they refer to the effect of numerics on features in the wave energy field, but they are not correct in reference to the effect of numerics on the gravity waves being represented. Nonspecific use of the terms in discussion of wave models should be avoided. Note that numerical error *can* (indirectly) lead to aphysical energy loss (or gain), for example, as energy is lost to absorbing boundaries via diffusion, or negative energy (which occurs occasionally due to wiggles) is set to zero by the wave model.

As part of a previous study (Rogers et al. 2002b), we conducted several numerical tests comparing the first-order, upwind, explict scheme of WAM and the QUICKEST scheme of WvW3 (among others). The results are intuitive enough that they do not need to be presented in detail here: the first-order scheme is demonstrated to be very inaccurate in situations where curvature in the wave field is large. The first-order upwind explicit scheme also has the unfortunate characteristic of *strongly* favoring propagation along computational grid axes (diffusion is reduced in these cases). The problem is typically reduced (slightly) by offsetting angular bins by half of the directional bin width ($\Delta\theta/2$). This tends to make diffusion large for all directional bins, as opposed to being large for all but a few axial bins. At 0(1°) geographic resolution, the QUICKEST scheme appears to be an excellent combination of accuracy and speed. Figure 1 compares the first-order scheme to the higher order scheme of WvW3.

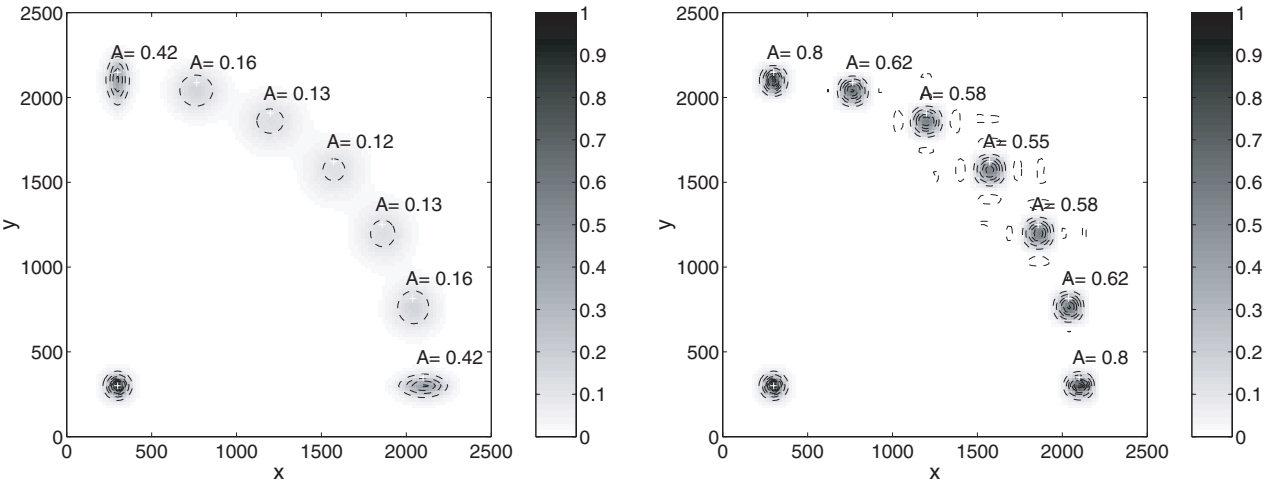

(a) First-order, upwind explicit

(b) QUICKEST

Fig. 1 — Results of two-dimensional spike propagation test. The conserved quantity (wave action density or wave energy density) is shown. Length scales are of arbitrary units; e.g., if units of km, the problem can be interpreted as swell propagation across an ocean. The narrow shape of the spike makes it a severe test case, very prone to the effects of diffusion and dispersion. Only one spectral bin is used per spike, so alteration of the shape of individual spikes during propagation is purely artificial. The spike is defined by: $N(x,y) = [\cosh(\Gamma / r)]^{-1}$, where r is a representative radius of the spike, and Γ is the radial distance from the spike center. Numerics are affected by Courant number, the resolution of the spike, and the angle of propagation. The initial shape and location of the spikes are shown in the lower left corner. The spikes are propagated at angles of 0, 15, 30, 45, 60, 75, and 90 degrees. The parameter "*A*" (shown at the end location of each spike) indicates the fraction of spike amplitude retained, a rough measure of diffusion (ideally, this number should be unity). The problem is non-dimensionalized and solved in terms of Courant numbers $C_{gx}\Delta t/\Delta x$ and $C_{gy}\Delta t/\Delta y$. Model parameters for the cases shown in this figure are: $C_g\Delta t/\Delta s = 0.6$, $\Delta x = \Delta y = 0.2$, where $C_g = \sqrt{C_{gx}^2 + C_{gy}^2}$ and $\Delta s = \sqrt{\Delta x^2 + \Delta y^2}$. Note that the QUICKEST scheme here is not identical to that of WvW3 insofar as it does not include the "ULTIMATE" limiter, which would be expected to remove "wiggles" in the solution (though it would also tend to "square" the features, see Tolman 2002c).

Geographic Resolution

Coarse geographic resolution leads to error. At NAVO and FNMOC, the global wave models use a 1° geographic resolution. This resolution is not adequate to represent the blocking by smaller islands (e.g., the Aleutians, French Polynesia, Hawaii). The error typically manifests as positive wave energy biases near such island groups. An approximate method for dealing with the problem of unresolved island groups has been implemented in an experimental version of WvW3 and will be included in the next release of the code. The method (and its origins) is described in Tolman (2001). In the far-field, it is debatable as to whether errors resulting from inadequate blocking by islands are large enough to be detected in comparisons to data.

Coarse geographic resolution also has an indirect numerical effect; numerical errors (namely, diffusion and dispersion in geographic propagation) are strongly affected by geographic resolution. Geographic resolution of wind forcing fields is unlikely to be a significant source of error, since forcing fields are generally well-described at provided (1°) resolutions. The description of small tropical storms is one possible exception.

Spectral Resolution

Coarse spectral resolution leads to errors. The NAVO and FNMOC models both use 24 directional bins ($\Delta\theta = 15°$) and 25 frequency bins (logarithmic distribution). Although this resolution is comparable to that used at other operational centers (see Bidlot et al. 2002, Table 1), it is quite coarse. This sometimes leads to aphysical discontinuities in swell fields (Fig. 2), which grow worse as the swell propagates. This is known as the "Garden Sprinkler Effect:" discrete spectral components appear as discrete geographic features in the wave model solution. Numerical diffusion tends to smooth these features (much as it smoothes numerical dispersion), so the aphysical features tend to be more evident in a model that uses a higher order geographic propagation scheme. WvW3 uses the diffusion technique of Booij and Holthuijsen (1987), which alleviates this to a large extent. Unfortunately, however, it tends to increase limitations on time step size (i.e., maximum Courant number tends to be smaller). The next version of WvW3 will include an alternative implementation of the Booij and Holthuijsen (1987) technique (one that does not restrict time step size, see Tolman 2002c).

In spectral space, as in geographic space, coarse resolution tends to increase numerical error.

Other Issues

Implementation issues, such as the handling of a model's diagnostic tail, limiters, source term integration, etc., can be expected to lead to errors and irregularities. (WAMDI Group (1988), Tolman (1992), Banner and Young (1994), and Hersbach and Janssen (1999) discuss these issues.)

Physical Formulations

Errors associated with inaccuracies of physical formulations occur at the generation stage of wave modeling, and (to a lesser extent) during the propagation stage. Physical effects during propagation (e.g., swell-to-wind momentum transfer) tend to be weak relative to effects during the generation stage, but occur over a longer duration.

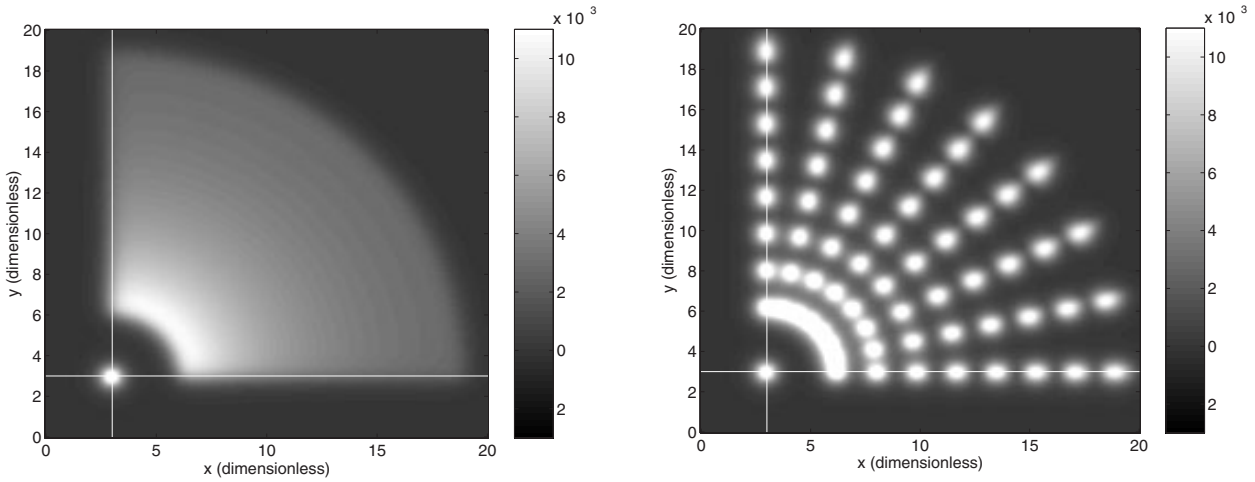

Fig. 2 — An energy field. All energy starts at the same location, shown in the lower left corner (the feature with center at x = y = 3). The problem is nondimensionalized using a method similar to that described in Fig. 1. Energy disperses as it propagates due to directional and frequency (i.e., speed) distribution of the initial spectra. (a) In this case, the spectrum is very finely resolved, so the Garden Sprinkler Effect is insignificant. The resulting energy field is continuous. (b) The discontinuity is a result of the Garden Sprinkler Effect. In this case, the spectrum consists of eight frequency bins and eight directional bins.

Wind Input S_{in}, and Dissipation S_{ds}

In all spectral wave models, the formulations used to represent input by wind forcing (TC also includes negative input by wind (wave-to-wind momentum transfer)), and decay by dissipative processes, although grounded in physical arguments, are notoriously empirical. This should not be construed as an aspersion on the developers of the formulations. The empiricism is required, in some cases, because our incomplete understanding of the physical processes involved, which is (in large part) limited by our inability to measure all (or even a significant portion of) relevant variables in the field. In other cases, the empiricism is necessary because we are representing small-scale processes (e.g., O(100m) features in the airflow) using a large-scale model. Also, we are approximating phase-associated processes (e.g., steepness-limited breaking) using a phase-averaged model. The dissipation term is particularly empirical, which is to a large extent a closure mechanism on the source/sink term balance.

Nonlinear Interactions S_{nl}

The physical process of nonlinear interactions is fairly well understood, and near-exact numerical techniques exist for computing these interactions. However, these near-exact techniques are computationally impractical for operational use. Thus, faster (but less accurate) approximations are necessary. Both WAM4 and WvW3 use the Discrete Interaction Approximation (Hasselmann et al. 1985). Informative discussions of nonlinear interaction formulations and their impact on wave models are found in Van Vledder et al. (2000) and Tolman (2002a).

Growth Curves

Canonical growth curves are appropriate for discussion here, since they are, for the most part, affected only by physical formulations. Numerical diffusion error is a negligible issue in canonical cases like those described here, since the curvature of the wave field (which is the relevant variable in the propagation scheme's truncation error) is generally very small. For similar reasons, resolution is

of lesser importance, compared to "real" simulations. Accuracy of wind forcing is obviously not an issue, since the winds are artificially prescribed. Implementation issues such as the handling of a model's diagnostic tail, limiters, etc., can be expected to cause some differences between WAM4 and WvW3 (see Tolman 1992, for example).

We compare three different physical formulations–TC physics with the WvW3 model; WAM3 physics (Komen et al. 1984, WAMDI Group 1988) with the WvW3 model; and WAM4 physics (Janssen 1989, 1991, Komen et al. 1994) with the WAM4 model–using a canonical growth case. Traditional canonical infinite-duration, fetch-limited growth curves are already presented for these models in the aforementioned references, so here we present a new type of comparison, the fetch-limited, duration-limited growth curve. In this section we also point out a significant discrepancy in the traditional usage of the "fully developed" sea state data set in model tuning.

A "fully developed" wave spectrum is given by Pierson and Moskowitz (1964) (henceforth denoted PM), as a function of wind speed, $U_{19.5}$. It is traditionally assumed (for example, in the landmark paper of Komen et al. (1984)) that wave models should approach this limit at their infinite-fetch, infinite-duration asymptote. The PM spectrum is based on the measurements of Moskowitz (1964). In that paper, Moskowitz gives approximate fetches and durations for the wind events corresponding to his "fully developed" wave measurements. Ideally, the models should reach their asymptotes at fetch, durations that (at least in a very approximate sense) agree with the fetches, durations given by Moskowitz (1964). However, this is usually not the case. For example, with the U_{10} = 15 m/s used in Komen et al. (1984), their chosen model reaches a nominal asymptote for a nondimensionalized fetch of around 10^8 (or greater). Here the nondimensionalized fetch is defined as $X_* = gX / U_*^2$, where g is gravitational acceleration, X is the fetch, and U_* is the friction velocity used by Komen et al. (1984) for the wind speed of U_{10} = 15 m/s: U_* = 0.64 m/s. See Komen et al. (1984) Fig. 8, lower panel. In fact, the nondimensional energy appears to be growing at its nominal asymptote. The fetches reported by Moskowitz for similar wind speeds, by contrast, correspond to nondimensionalized fetches typically in the range of $4 \times 10^6 - 10^7$. (In Moskowitz (1964), for wind speeds of 28-32 kts, the fetch given is in the range of 100-225 nmi.) Thus, in this case, there is a major discrepancy between the data set and the way that it is applied in the model. One can expect that for similar wind speeds, wave growth in such a model would be too slow.

Figure 3 shows fetch-duration growth curves for the three models. (Similar comparisons were made for the SWAN model (Simulating WAves Nearshore, Booij et al. 1999) by Rogers et al. (2002a). Two of these are reproduced, in slightly different format, in Appendix A.) Because the models do not scale in the same manner as the PM spectrum, we do not present the curves in nondimensionalized form. We choose the wind speed of U_{10} = 15 m/s for this canonical case, since it is the higher winds speeds (12-25 m/s) that generate low-frequency energy. The PM wave height for this wind speed is 5.5 m. The fetch/durations reported by Moskowitz (1964) are also shown on the figure. Note that the fetch/durations given by Moskowitz are approximate and do not represent growth from a near-zero wave condition (see Moskowitz (1964), p. 51-64), whereas the model simulations do start at a near-zero wave condition. Thus, one might expect that 0(10%) should be added to the fetch/durations of the Moskowitz values to allow direct comparison to the models. Even so, the models are clearly not reaching the fully developed wave height quickly enough. The WAM Cycle 3 physics are exceedingly poor in this regard, whereas the TC physics are the "best" in the group.

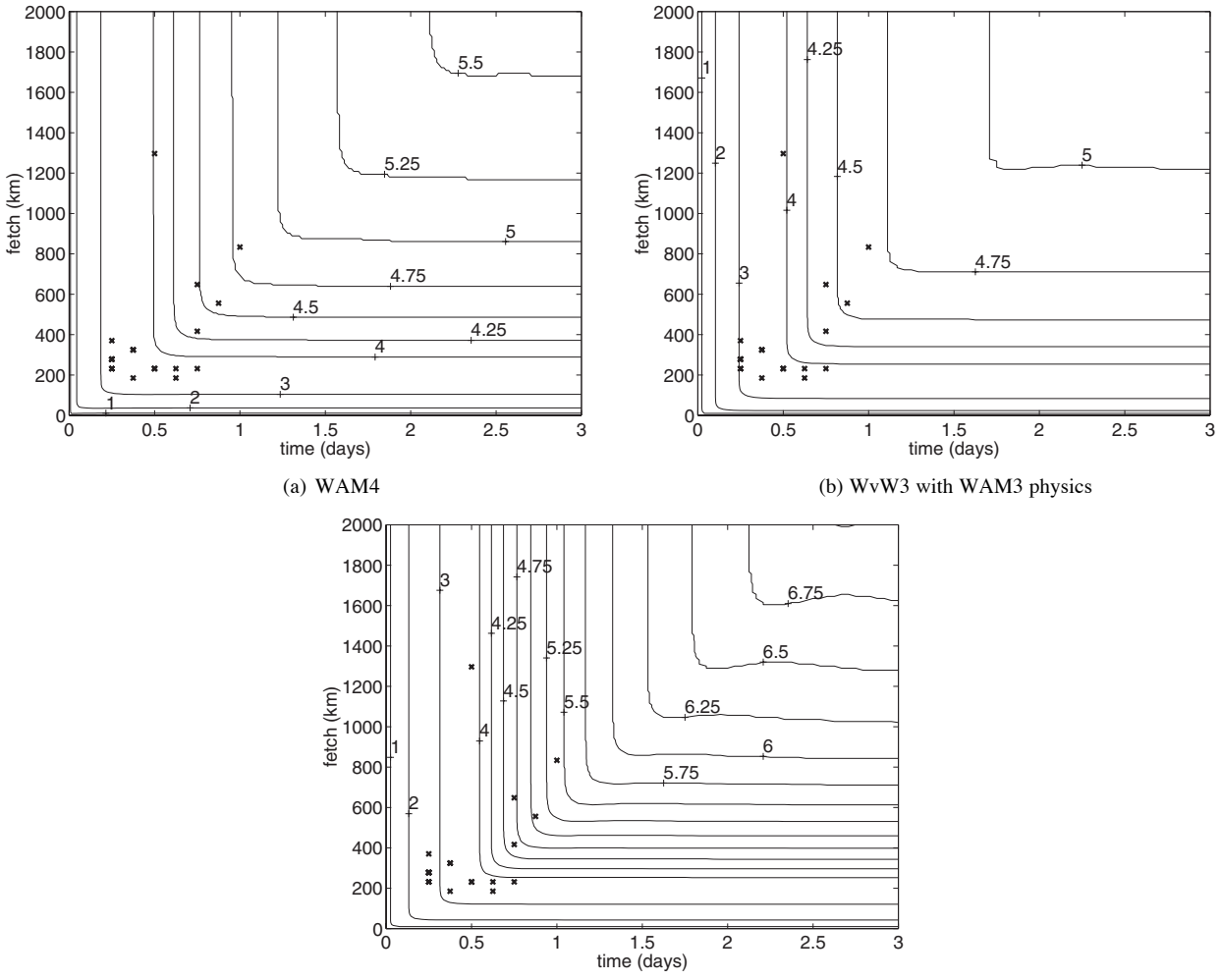

(a) WAM4

(b) WvW3 with WAM3 physics

(c) WvW3 with TC physics

Fig. 3 — Fetch-limited growth curves of the three models. Wave height (m) as a function of fetch and time are shown for the case of infinite depth and U_{10} = 15m/s. The Pierson-Moskowitz spectrum predicts a wave height of 5.5 m for this wind speed. The duration and fetches reported by Moskowitz (1964) are indicated (i.e., the models should produce a wave height of approximately 5.5 m at the locations of the x's). Note, of course, that events measured by Moskowitz did not start in a state of rest, as is the case with the models.

Because of the uncertainty related to the Moskowitz fetch/duration values, it is probably unwise to lend too much importance to comparisons to these values. However, the nature of the growth curves themselves (in the absence of data) gives us considerable insight into the underlying nature of the models: the behavior of the models under the much-simplified circumstance of a constant, uniform wind field, without complicating issues such as diffusion, multiple sea states, and the accuracy of forcing. Note, for example, that WAM4 tends to be more energetic in the short-fetch (less than 200 km in this case) and short-duration (less than 12 h) regimes, whereas for longer fetch/durations, WvW3 is more energetic. (For comparison, the difference between the WvW3 and WAM4 result is shown in Fig. 4.) This is interesting in light of the fact that in comparisons by Tolman et al. (2002), WvW3 tended to be more energetic than WAM4. This can be found in Tolman et al. (2002), pg. 318, second column. In their comparisons, different wind forcing is used for the two wave models, but the authors feel that this difference in wave model result (WAM having a regression slope that is too low, and WvW3 having a regression slope that is too high) is too large to be attributed to wind forcing alone. Also note that the contours of Fig. 3 tend to be parallel to the axes: this indicates that under most circumstances, the models are either fetch-limited or duration-limited, rarely both.

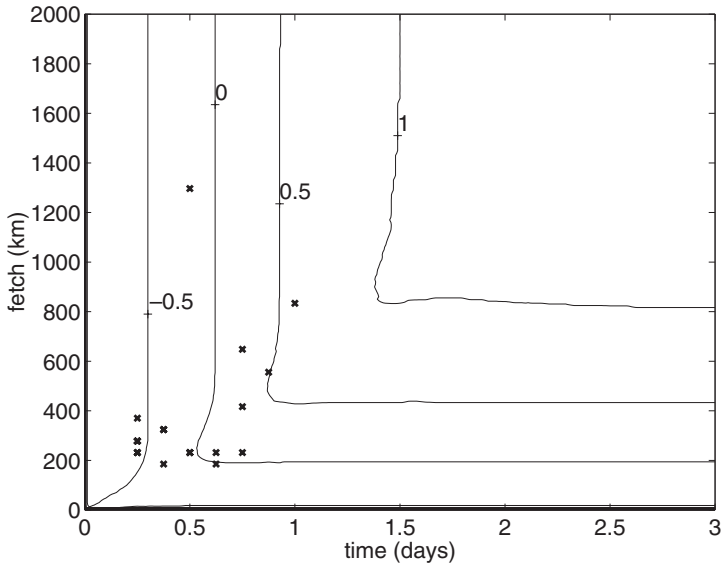

Fig. 4 — As Fig. 3, except that the difference between 3(a) and 3(c) are shown ($H_{m0,TC} - H_{m0,WAM4}$) (m).

The dramatic difference between the model results with three physical formulations (WAM3, WAM4, TC) suggest that, in practice, error associated with physical formulations may be quite significant (since two very different results cannot both be "correct"). It is debatable with regard to what fetch/duration regions of Fig. 3 are most relevant to global modeling. Most likely, the regions wherein the Moskowitz measurements fall are very relevant, but this is complicated by the nonstationarity and nonuniformity of storm events, as well as the complexity of sea conditions prior to storm events and how this impacts growth during the storm (i.e., initial conditions).

With regard to the growth characteristics of third-generation wave models, most of the author's experience is not with WAM or WvW3, but with the wave model SWAN. This model, although it can be used effectively for global wave modeling, is computationally inefficient at such large scales (Rogers et al. 2002b). Thus, it is unlikely to ever be applied globally in Navy operations. However, since the models share many similarities, insights into SWAN can still be useful in understanding WAM and WvW3. We describe some of our investigations of the growth characteristics of SWAN in Appendix A.

Forcing

Inaccuracies in the wind forcing used by a global wave model are another source of error. Several studies have dealt with the accuracy of wind forcing from the perspective of the wave modeler, e.g., Komen et al. (1994), Cardone et al. (1995), Cardone et al. (1996), and Tolman (1998). (Persons interested in reading Tolman (1998) should be aware that the modifications to NCEP wind fields described in Tolman (1998) are no longer used, since they are now deemed unnecessary (see Tolman et al. 2002).) However, up to now, no such study has been conducted with regard to the Navy's atmospheric model/wave model system. This work has now been done, using global wave model hindcasts with different wind forcing models (Section 5). In this section, we perform some preparatory investigation by looking into the accuracy of the wind forcing directly.

As mentioned above, only high wind speed events generate low-frequency energy in large quantities. (Lower wind speed conditions (e.g., U_{10} = 3-8 m/s) are not directly relevant to this study.) It is

crucial that the wind forcing fields accurately capture the size, duration, and intensity of these stronger wind events. Such wind events are most common in the winter seasons. We make two regional comparisons here, both relevant to low-frequency wave energy measured by buoys along the California coast.

The Atmospheric Models

We include two wind analysis sources in our comparison: NOGAPS (Navy Operational Global Atmospheric Prediction System, see, e.g., Hogan and Rosmond (1991) and Rosmond et al. (2002)) analyses and NCEP analyses (see, e.g., Kanamitsu 1989 and Caplan et al. 1997), which are products of the GDAS (Global Data Assimilation Scheme) and the MRF (aviation cycle of the Medium Range Forecast) model. The NOGAPS analyses were obtained from NRL archives (maintained by Pamela Posey (NRL) and Kelley Miles (Sverdrup Technologies, Stennis Space Center, Mississippi). The NCEP wind analyses are provided via free, anonymous ftp by NCEP. The NOGAPS is used by the operational Navy (FNMOC and NAVO) to force the global wave models (WvW3 and WAM4, respectively), so its relevance to this study is obvious. The GDAS/MRF model is used to force NCEP's operational global wave model (WvW3). It is included to compare the Navy's operational product with another "mainstream" operational product. The ECMWF (European Center for Medium range Weather Forecasts) and the UK Meteorological Office also run comparable wave models, forced by comparable atmospheric models, that could be used for comparison (see e.g., Bidlot et al. 2002); unfortunately, these analyses are less accessible than those of NCEP.

Northern Hemisphere Winter

First, we look at wind field accuracy in the northeast Pacific Ocean (Fig. 5) in January 2001. During winter in the north Pacific, storm systems, generally traveling from west to east, irradiate much of the basin with swells. When these swells reach the California buoys, they are still relatively young. Figure 6 and Table 1 compare the wind speeds from the two models to L3 QSCAT data for the semi-circular region shown in Fig. 5, for the duration of January 2001. Figure 7 presents a short time-series comparison at the buoy location indicated in Fig. 5. The L3 QSCAT data, shown in Fig. 7, provide a sanity check on the ground truth used in Fig. 6. In the scatterometer comparisons, we see that both models are biased low at high wind speeds, with the NOGAPS model exhibiting greater bias (and greater scatter as well). In the buoy comparison, NOGAPS badly misses the peak of the strong wind event measured on January 10-12. Figure 8 shows scatter plot comparisons to the buoy data for the entire month. Again, the negative bias at high wind speeds is evident.

Southern Hemisphere Winter

Second, we look at wind field accuracy in the southern Pacific Ocean (Fig. 9) during July 2001. At this time of year, strong storms in this region generate large quantities of low-frequency energy, some of which is directed toward Hawaii and the continental U.S. coastline, where these swells are measured by National Data Buoy Center (NDBC) buoys. Figure 10 and Table 2 compare the two models to QSCAT measurement in the semi-circular region shown in Fig. 9 for the duration of July 2001. Again, the NCEP model outperforms NOGAPS, but both models are biased low at high wind speeds. Interestingly, the models appear to be performing better here than in the north Pacific case, where buoy data are available for assimilation into the models.

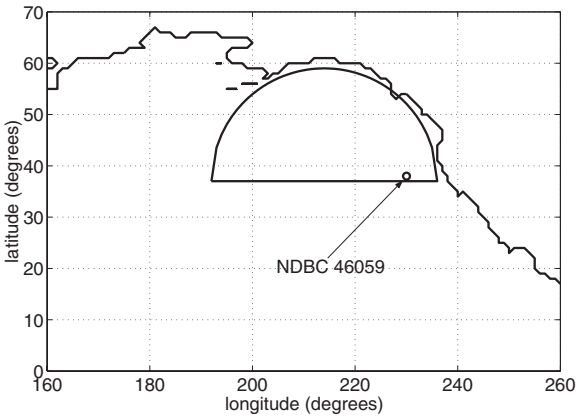

Fig. 5 — Location of region of northeast Pacific Ocean used in comparisons of atmospheric models to scatterometer data. The location of NDBC buoy 46059 is also indicated.

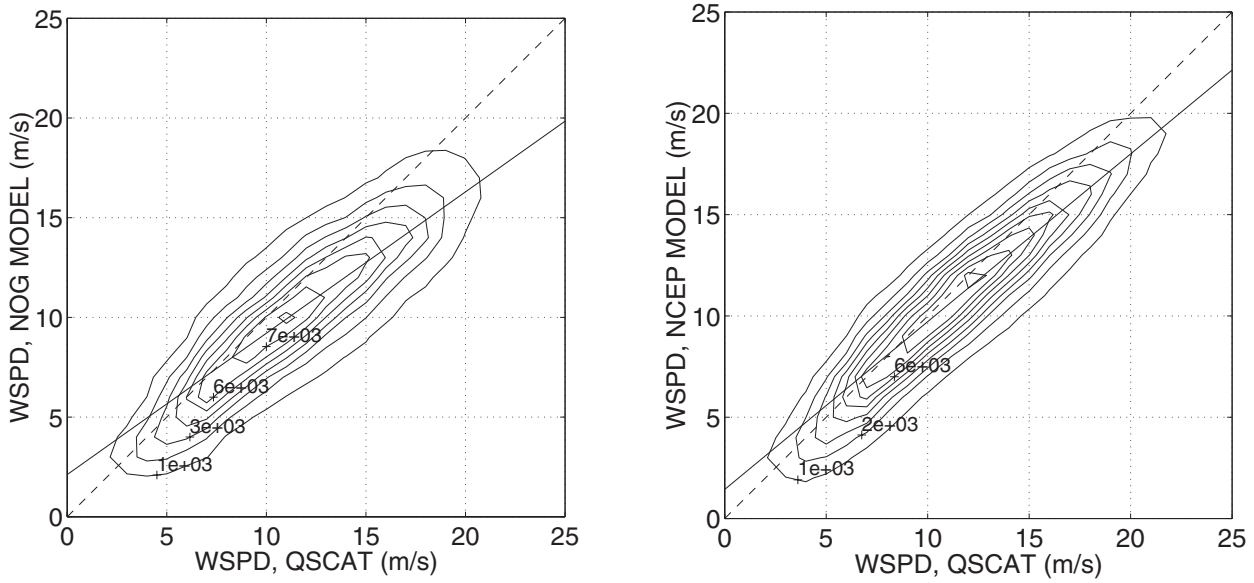

(a) NOGAPS model (b) NCEP model

Fig. 6 — Scatter plot comparisons of atmospheric model vs scatterometer data for region indicated in Fig. 5 and duration of January 2001. Contours denote number of occurrences in a 1.0 × 1.0 m/s square. Wind speed is the 10-m elevation scalar quantity. Solid line indicates regression. Dashed line indicates perfect match.

Table 1 – RMS error, regression slope, regression y-intercept, and bias (mean error) for the two models in the north Pacific wind validation. The root-mean-square (RMS) error and regressions given are based on the entire range of wind speeds; the bias is only the high wind speed bias ($U_{10,measured} > 12$ m/s).

Model	RMS Error (m/s)	Slope	Y-intercept (m/s)	Bias (m/s)
NOGAPS	3.21	0.71	2.12	–2.77
NCEP	3.1	0.83	1.44	–1.52

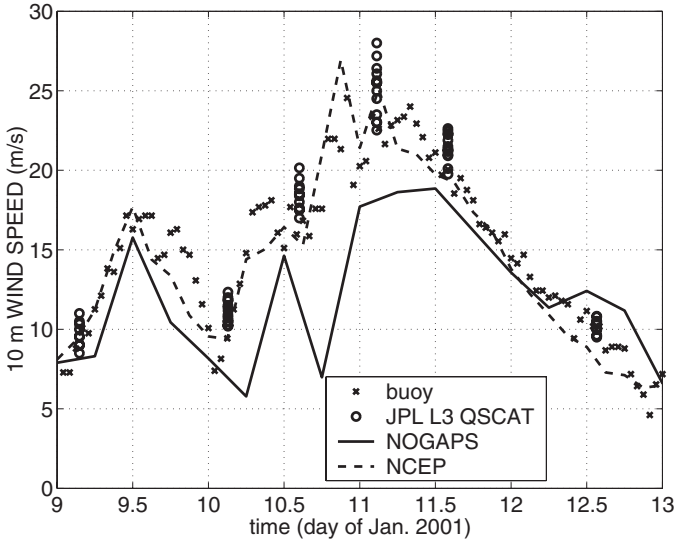

Fig. 7 — Time series comparison for a short period of January 2001 at location of NDBC buoy 46059. Wind speed is the 10-m elevation scalar quantity.

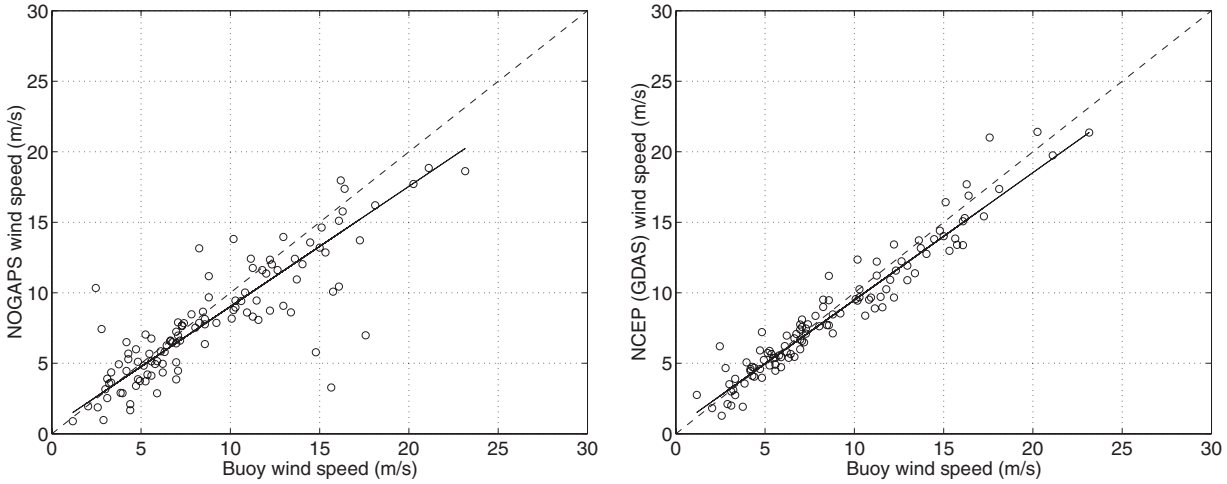

(a) NOGAPS (regression slope = 0.85, RMS error = 2.7 m) (b) NCEP model (regression slope = 0.90, RMS error = 1.2 m)

Fig. 8 — Scatter plot comparisons of atmospheric model vs. NDBC buoy 46059 data for the period of 0000UTC January 1 2001 to 0600UTC January 28 2001.Wind speed is the 10m elevation scalar quantity. Solid line indicates regression. Dashed line indicates perfect match.

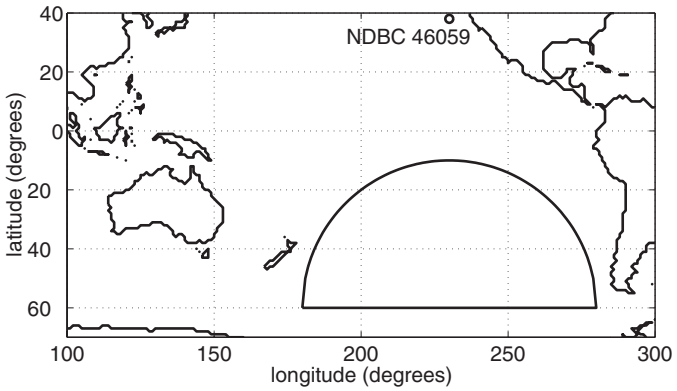

Fig. 9 — Location of region of Southern Pacific Ocean used in comparisons of atmospheric models to scatterometer data

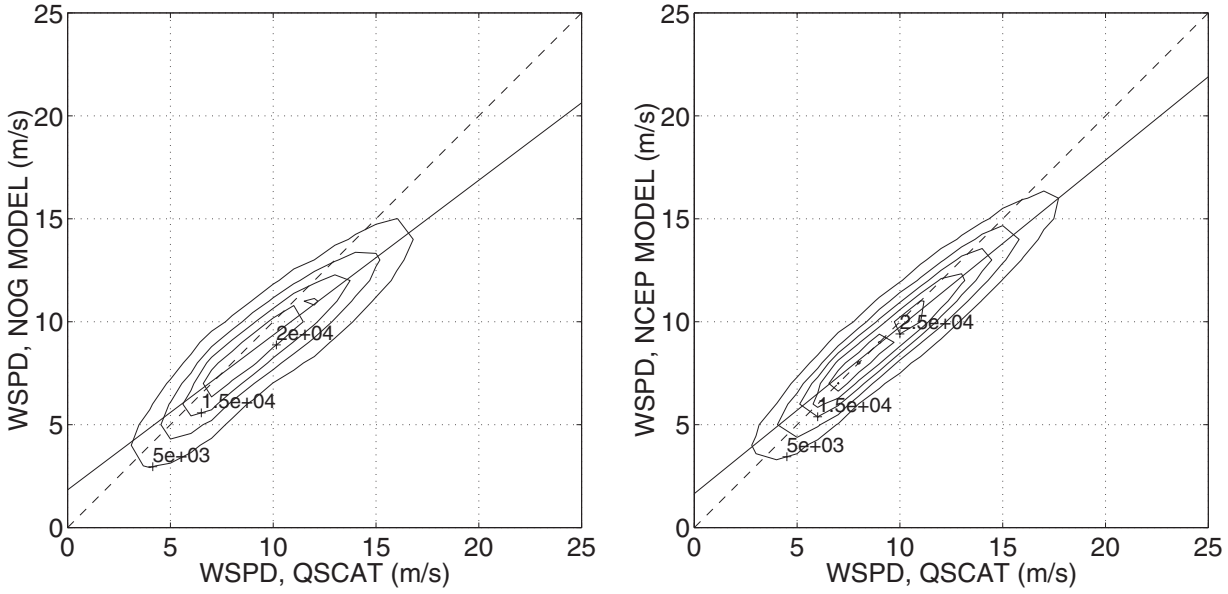

(a) NOGAPS model (b) NCEP model

Fig. 10 — Scatter plot comparisons of atmospheric model vs scatterometer data for region indicated in Fig. 9 and duration of July 2001. Contours denote number of occurrences in a 1.0 × 1.0 m/s square. Wind speed is the 10-m elevation scalar quantity. Solid line indicates regression. Dashed line indicates perfect match.

Table 2 – RMS error, regression slope, regression y-intercept, and bias (mean error) for the two models in the southern Pacific Ocean wind validation. The RMS error and regressions given are based on the entire range of wind speeds; the bias is only the high wind speed bias ($U_{10,measured} > 12$ m/s).

Model	RMS Error (m/s)	Slope	Y-intercept (m/s)	Bias (m/s)
NOGAPS	2.51	0.75	1.83	−2.43
NCEP	1.72	0.81	1.65	−1.41

Atmospheric Model Results: Discussion

These two comparisons suggest that (a) NOGAPS has a tendency to underpredict high wind speeds, and (b) NOGAPS is not as accurate as the comparable operational product of NCEP (with regard to both high wind speed bias and scatter). However, since this comparison is rather limited (being only two regions of the Pacific and only two months of comparisons), we should not draw conclusions on this alone. Fortunately, extensive validations against buoy data are published by FNMOC, grouped by month and by region (where buoys exist). These comparisons also indicate a negative bias at high wind speeds, although the magnitude of the bias varies considerably by region. These comparisons can be found at http://www.fnmoc.navy.mil/PUBLIC/MODEL_REPORTS/MONTHLY_MODEL_SUMMARY. (Unfortunately, they are not published in print.) The January 2001 regional comparisons for the Gulf of Alaska and northeast Pacific regions show only a slight negative bias at high wind speeds (buoy 45059, shown in Fig. 4 here, is in the latter group). The "British Columbia-Canadian" and "Oregon-Washington" regions show moderate negative bias, while the "northern California" and "southern California" buoy groups show very dramatic negative bias. During January 2001 and July 2001, in the "Hawaii" region, winds (which are the typically weak-to-moderate equatorial winds) are reasonably well predicted, but the wave models are generally underpredicting larger (3-6 m) wave heights. This may be a result of underprediction of swells due to underprediction of high wind speeds in the north Pacific and Southern Ocean, respectively.

It is important to put our discussion of the NOGAPS model in context, since this investigation should not be interpreted as a general condemnation of that model. This investigation is only looking at one rather small aspect of the NOGAPS model, the aspect of the model that is most relevant to low-frequency energy: the prediction of strong wind events in surface (10-m) wind speed analyses (nowcasts). The model does not appear to have the same degree of bias at low-to-moderate wind speeds. It is possible that other model predictions, such as 500-mb wind speeds and precipitation are much more accurate. It is possible that the forecasts tend to be more energetic than the analyses, so bias in forecasts might be smaller. (We concentrate on the wind analyses, since it is the wind analyses (not forecasts) that generate swells in the wave model (including young swells), which tend to dominate the low-frequency portion of measured spectra.) Underprediction of high wind speeds tend to be associated with computational geographic resolution. The NCEP model uses a higher resolution than NOGAPS, so the skill differences may be (to some extent) a result of available computational resources, rather than model design. And of course, model skill is always in flux. The Navy is now implementing an improved atmospheric data assimilation system (Navy Data Assimilation System (NAVDAS), Daley and Barker 2001). NAVDAS is discussed later in this report.

Potential Sources of Error: Discussion

Thus far, we have discussed and illustrated several potential sources of error in global wave modeling. However, none of this provides much insight regarding the relative importance of these errors in practice. For instance, one might look at Figs. 11, 12(a-c) and conclude that these models are doing a poor job of hindcasting low-frequency energy in these cases, but one would have no indication of the reason for this. In Section 5, we investigate this issue through the use of global hindcasts.

Here, we do not investigate every potential source of error (e.g., we do not investigate the impact of the handling of the high-frequency tail), but focus on those issues that might reasonably be expected to have significant impact on modeled integrated parameters (e.g., low-frequency wave height) in oceanic-scale models.

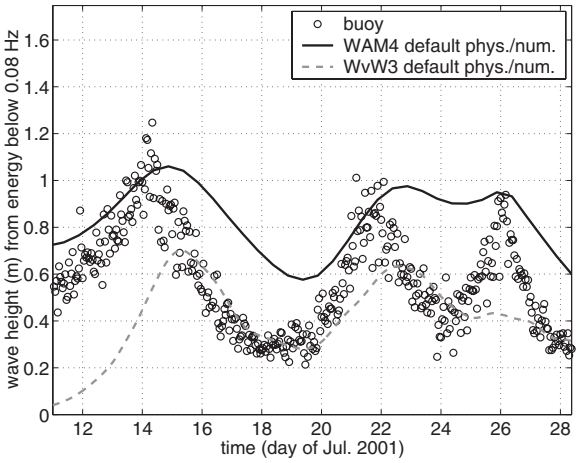

Fig. 11 — Comparison of low-frequency wave height: two models (WAM4 and WvW3) vs buoy measurements. Location is NDBC buoy 46059 (west of San Francisco). Both models use their respective default physics and numerics, and both models are forced by the NOGAPS atmospheric model analyses. WAM4 analysis archives were provided by Larry Hsu (NRL).

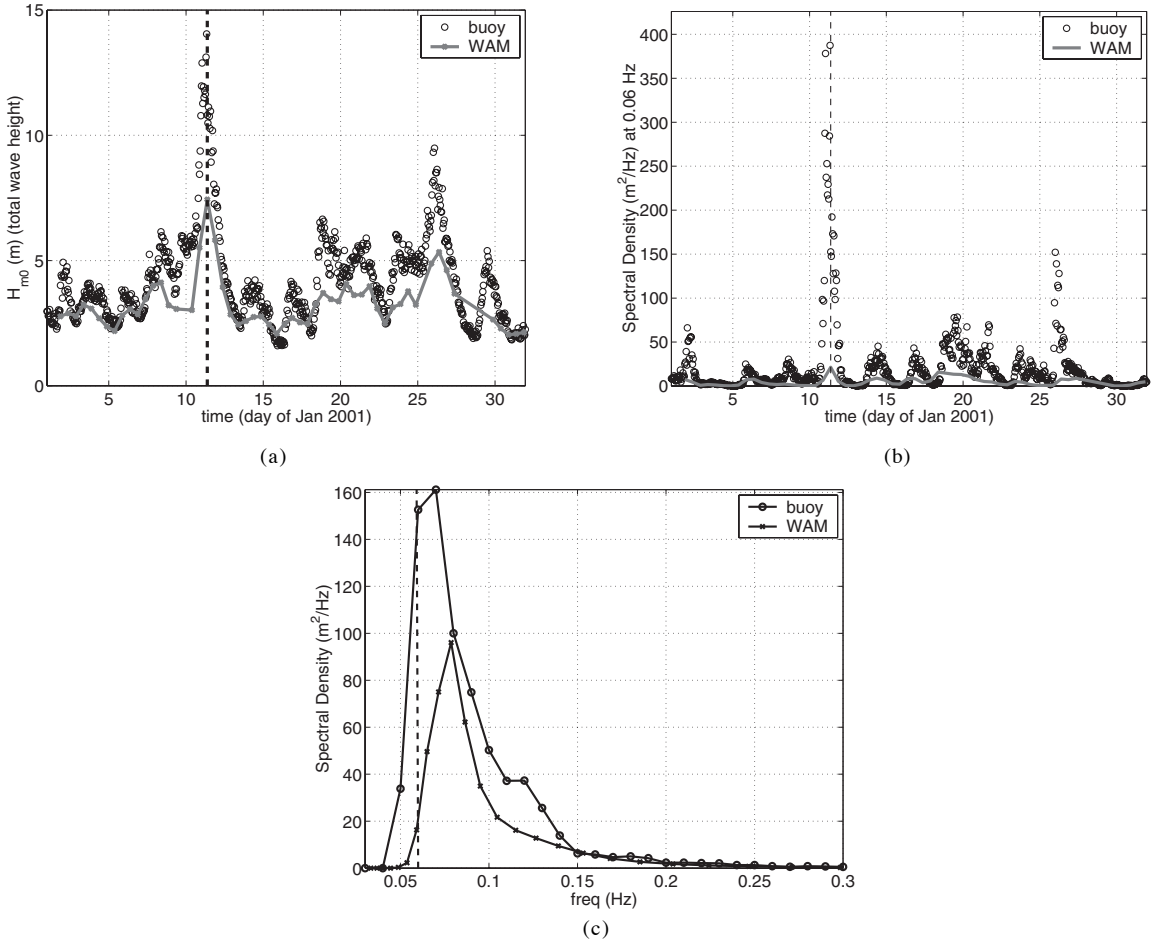

Fig. 12 — Comparison of WAM vs buoy measurement at location of NDBC buoy 46059 (deep water offshore of San Francisco). The WAM4 analyses were provided by Larry Hsu (NRL). (a) Time series of zero moment wave height during January 2001. Wave height is energy-based, calculated from frequencies 0.03 to 0.33 Hz. The dashed vertical line indicates the instant in time that is plotted in (c). (b) Time series of 0.06 Hz spectral density during January 2001. The dashed vertical line indicates the instant in time that is plotted in (c). (c) Frequency distribution; time shown is January 11, 2001, at 0900Z. The dashed vertical line indicates the frequency that is plotted in (b).

4. ALTERNATIVE WIND FORCING FOR HINDCASTS: DATA-DERIVED WIND FIELDS

We have introduced two operational global wind products: the FNMOC product (NOGAPS) and the NCEP product (AVN/GDAS). Both of these were readily available to us and can be used to force global wave model hindcasts. During the wind forcing validation (described in Section 3), it became apparent that the extensive coverage of the QuikSCAT data-set makes it possible to derive snapshot wind fields by using that data set, which could be used to force a wave model.

Existing Products

The creation of data-derived fields is not new. In fact, Schlax et al. (2001) provide a detailed analysis of sampling errors associated with the creation of these wind field maps, with oceanographic models mentioned as one possible target application. The Navy Data Assimilation System (Daley and Barker 2001), presently in transition to FNMOC, will be used to create similar wind field maps, although this feature will not be included in the operational NAVDAS initially, and it is uncertain when it will be implemented.

One such product is presently available, the Florida State University (FSU) Center for Ocean-Atmospheric Prediction Studies (COAPS) provides snapshot wind fields based on QuikSCAT data (Pegion et al. 2000). These are freely available by anonymous ftp. However, comparisons to buoy data and JPL QSCAT data indicate that these wind fields are probably not appropriate to use as forcing of a global wave model (Fig. 13). Note that this does not suggest a problem with the data set itself, merely that it was not designed for this type of application.

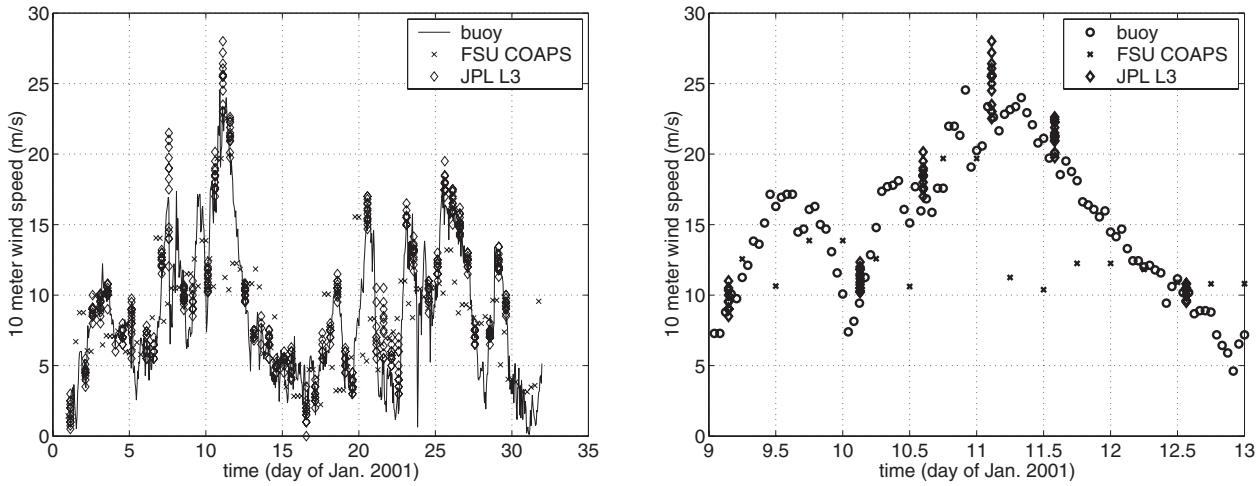

(a) Entire month of January 2001 (b) January 9-13, 2001

Fig. 13 — Comparison of three different data types at location of NDBC buoy 46059: buoy data vs FSU COAPS data vs JPL L3 data. In the case of the L3 data, measurements taken within 0.5° of the buoy location are plotted.

Map-generation Method

Description

We therefore created our own data-derived wind fields on a uniform space-time grid, for the specific application of forcing a global wave model. Because of time constraints, this was done by using a relatively simple method. At time t (corresponding to the time of the snapshot map, which is calcu-

lated at 3-h intervals), longitude λ, and latitude φ (corresponding to a point in the forcing grid), the wind vector is calculated using the following logic:

1. If a JPL L2B measurement is nearby (in time and space), use that measurement.
2. Otherwise, use NOGAPS value for that time/location.

NOGAPS is used in the "gap-filling" role here (as opposed to NCEP fields) because of potential for eventually using an evolution of this system operationally. (The use of NCEP wind fields by the Navy, operationally, has disadvantages unrelated to model skill.) The L2B data set is used, rather than the L3 data set because the latter data set contains data gaps associated with rain occurrence, whereas the L2B data includes all data points, regardless of quality. (In our case, we expect that having data gaps is potentially more harmful than having locations where data are of questionable quality.) We did use the L3 data in some preliminary hindcasts (where indicated in Section 5).

The definition of "current" (nearby in time) is subjective. Clearly, one's tolerance of temporal errors will depend on the severity of the bias in the model that is used as the background: one would not want to pollute an accurate atmospheric model analysis with measurements that differ from the time of the analysis by several hours. One the other hand, if model bias is severe (which appears to be the case with high wind speeds in NOGAPS), one might choose to be more aggressive with usage of measurements. Figure 14 shows coverage of QuikSCAT data with varying level of data usage. We chose the "within 6 hours (12-h window)" criterion for data usage, since that provides reasonably good coverage of the ocean's surface. We applied two other windows to hindcasts, to investigate impact on wave model performance. This is described in Section 5.

Another subjective issue is the "smoothness" of the resultant wind vector map. A wind field with a large degree of nonuniformity and nonstationarity does not present problems (e.g., with stability or consistency) for a wave model such as WAM or WvW3. Since WvW3 uses a dynamically adjusted source term time step, it is conceivable that having irregular wind fields might increase computation time. We checked the run times of one of our hindcast cases (January 2002, see Section 5). The simulation with QuikSCAT/NOGAPS forcing required 2-3% more computation time than the simulation with NOGAPS forcing. Thus, it is not necessary to smooth wind fields. In fact, smoothing would very likely have a negative impact on model performance, since this would tend to reduce higher wind speeds. Similarly, wind curl, critical to other types of models, is much less important to wave model forcing.

The "meteorological correctness" of fields derived from data in this manner is, of course, rather dubious. From the point of view of the wave model, this may not be relevant. Measurement error and sampling error (e.g., Schlax et al. 2001) are the more relevant issues, since they more directly separate the product from "truth."

Potential Improvements

Clearly, this is a very simplistic method of creating snapshot wind fields. There are a number of ways to add sophistication. Some of these methods—for example, two-dimensional variational methods (see Atlas et al. (1996), Pegion et al. (2000))—may be undesirable due to reduction of peaks. (This is speculation; we have not yet investigated these techniques.) Other improvements are probably less problematic: for example, the transition from NOGAPS to scatterometer data might be made more gradual, by including a weighting function based on the temporal error of the measurement (error being the difference between measurement time and snapshot time). The weighting function might also vary according to the bias of the atmospheric model, which (one would expect) would vary by geographic location and season.

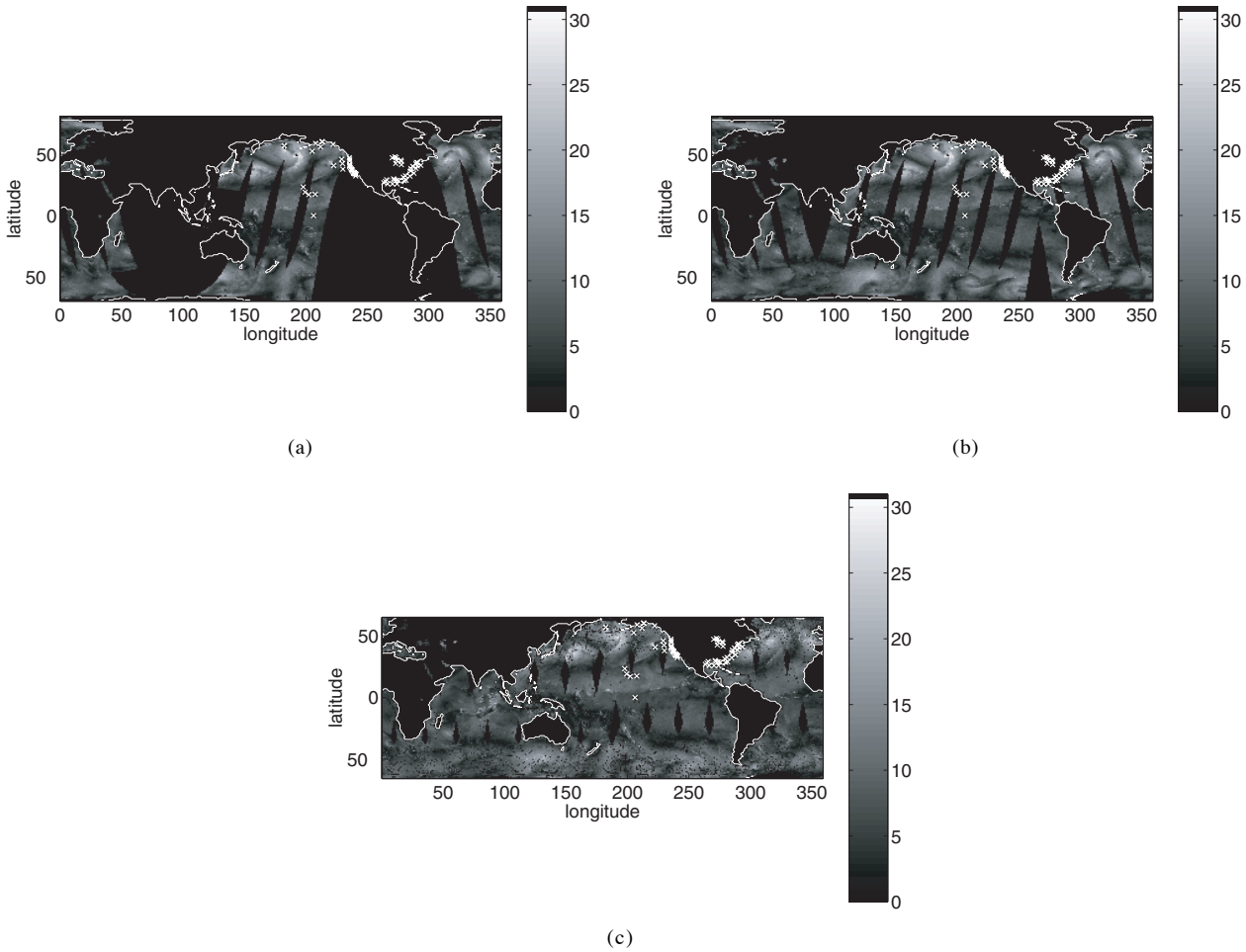

Fig. 14 — Wind field map created from QuikSCAT data (wind speed, m/s). The time of the "snapshot" shown is January 28, 2001 at 0600 UTC. In all cases, NOGAPS forcing would be used to fill in gaps (where data are not used), but are shown as blank areas here. (a) L2B, W3: QuikSCAT L2B data within 3 h of snapshot time (before or after) are included in snapshot. (b) L2B, W6: L2B QuikSCAT within 6 h of snapshot time (before or after) are included in snapshot. (c) L3, W12: L3 QuikSCAT within 12 h of snapshot time (before or after) are included in the snapshot. In (c), note the smaller gaps in the Southern Pacific Ocean, unrelated to swath coverage. These occur in the L3 data and are associated with rain. (The L3, W12 wind field was not applied in hindcasts.)

Another obvious improvement would be the inclusion of additional data–for example, buoy, ADEOS-2 scatterometer (November 2002 planned launch date), altimeter (e.g., TOPEX), and SSMI (Special Sensor Microwave/Imager). Of course, each new remote sensing data set would need to be validated against in situ data prior to inclusion.

5. HINDCASTS

Propagation Error Investigation

For the investigation of error accumulating during propagation due to numerics and coarse resolution, we have an uncommon advantage: a near-exact model that can be used for hindcasts: the Navy Swell Model (Version 1).

Swell Model: Description

The Navy Swell Model was developed at the Scripps Institution of Oceanography (W. O'Reilly) and the Naval Research Laboratory at Stennis Space Center (L. Hsu). Where WAM and WW3 are Eulerian (finite-difference) models, the Navy Swell Model is Lagrangian, using backward ray tracing for propagation. Thus, propagation inside the Swell Model can be considered near-exact. No source/sink terms are calculated internally. The Swell Model takes any WAM action density spectra field (which is contained in a WAM restart file) and propagates it forward to a user-specified arrival location. The Swell Model uses very fine resolution of topography (5 min) and wave direction (1°). If the Swell Model grabs swell energy when it is relatively young (e.g., 1 day old) and propagates it forward several (e.g., 8) days, then much of the propagation is free of effects from the WAM model's relatively poor numerics and resolution. A 1-day forecast from the Swell Model, on the other hand, will have only one day of "error-free" propagation. Of course, there is a limitation to the utility of such an approach: a 6-day old swell field will not be captured in a 10-day Swell Model forecast, since the wave energy would not have been generated yet in the WAM restart file that is used to generate the forecast.

To summarize, differences between the Swell Model and WAM model can be due to one of two things: (1) inaccuracies in the WAM model associated with numerics and resolution, or (2) the wave event is not "old" enough to be represented in the Swell Model forecast. These two cases are, in general, easy to distinguish, giving us an excellent technique for quantifying errors related to numerics and resolution.

Note that the Swell Model and WAM produce two separate forecasts. (Their output cannot be combined in a meaningful and consistent manner.)

Swell Model: Application Descriptions

Figure 15 shows a time series comparison of energy density at 0.06 Hz at the NDBC buoy offshore of Monterey during May 2001. In this case, there is a series of four swell events, all generated in the southern Pacific Ocean, arriving at the California coastline. The WAM model analysis is compared to the 8-day Swell Model forecast. In this case, the Swell Model is taking the WAM analysis restart file corresponding to 8 days prior and propagating it forward to this location. The buoy data are also shown. However, they are not relevant to this particular discussion, since we are only interested in determining the magnitude of the effect of numerics and resolution in the WAM model. We see that the diffusion effects in WAM are quite significant with these relatively old swells. If one compares the low-frequency wave height of these swell events rather than spectral density, the impact is less dramatic (Fig. 16), since the frequency integration blurs the time series. Here, the faster waves of later swell events are actually overtaking the slower waves of previous events. Figure 17 shows a longer time series of the same low-frequency wave height, for the same location. In general, there is not a great deal of difference between the Swell Model and the WAM model in this comparison. Note that any wave event that shows up in the Swell Model forecast is a swell event older than the forecast time (8 days in this case). It is quite surprising that despite being propagated over such long distances, the apparent effect of diffusion (and other numerics/resolution inaccuracies) is so small.

As a demonstration of repeatability, we show another Swell Model comparison (Fig. 18). This time, we look at a different buoy and different time (although still a swell event in summer time at the coast of California). The apparent impact of diffusion on low-frequency wave height is again quite small. Several other comparisons were made which are not presented here. In general, they were qualitatively similar to comparisons presented.

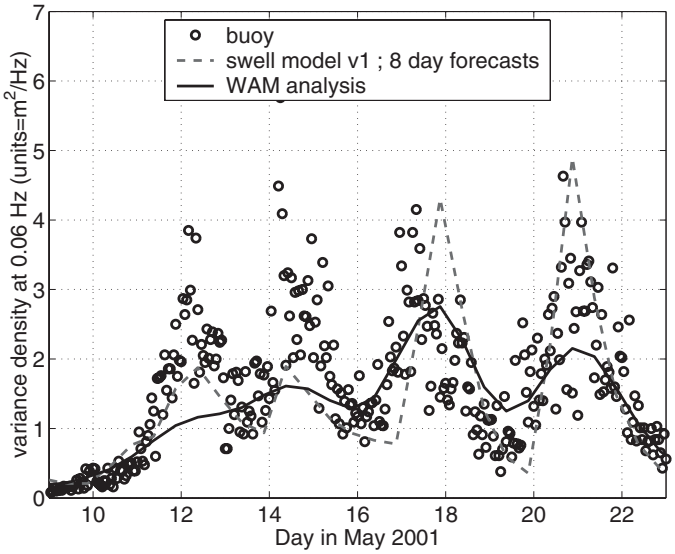

Fig. 15 — Comparison of Navy Swell Model (8-day forecast) vs WAM analysis vs buoy data at location of NDBC buoy 46042 (outside Monterey Bay). Spectral density at 0.06Hz is shown. Time period is May 2001. WAM4 analysis archives and swell model simulations were provided by Larry Hsu (NRL).

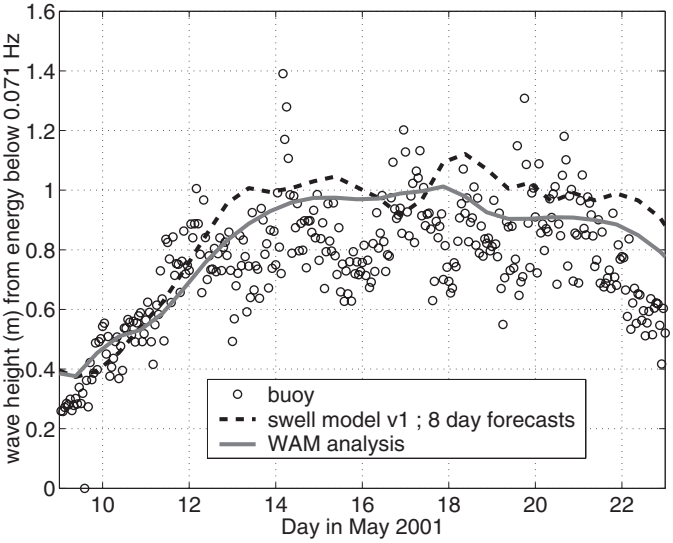

Fig. 16 — Same as Fig. 15, except low-frequency wave height is shown (energy up to 0.071 Hz). WAM4 analysis archives and swell model simulation were provided by Larry Hsu (NRL).

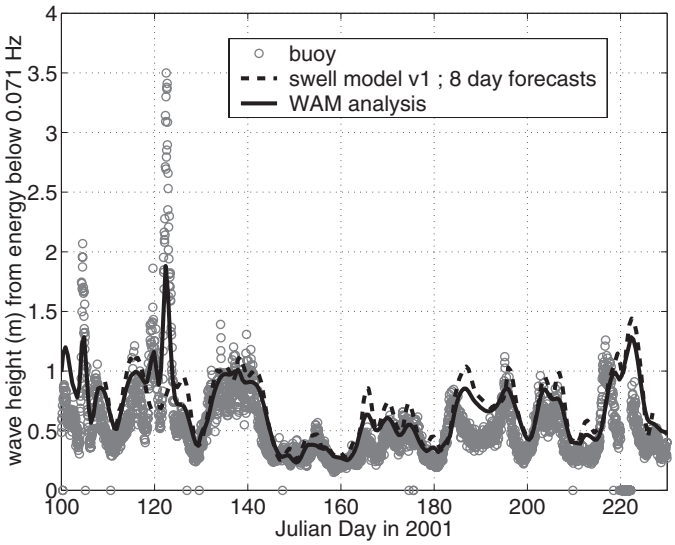

Fig. 17 — Same as Fig. 16, except longer time series (entire summer of 2001) is shown. May 14 2001 is Julian Day 134. WAM4 analysis archives and swell model simulation were provided by Larry Hsu (NRL).

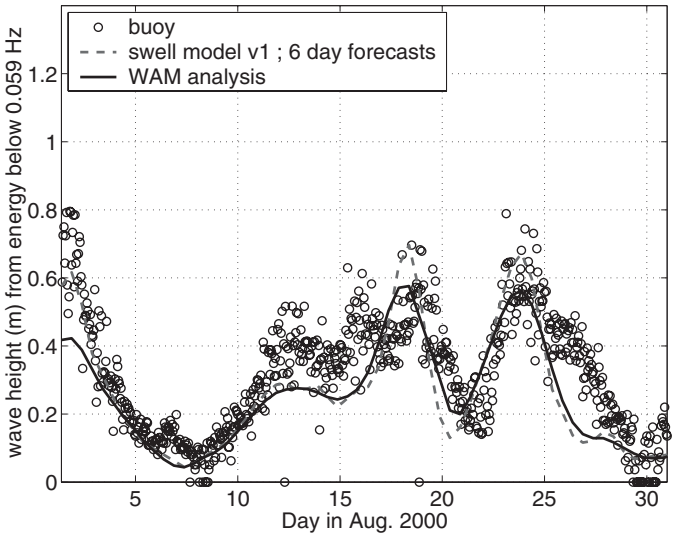

Fig. 18 — Comparison of Navy Swell Model (6-day forecast) vs WAM analysis vs buoy data at location of NDBC buoy 46059 (offshore of San Francisco). Low-frequency wave height is shown (energy up to 0.059 Hz). Time period is August 2000. WAM4 analysis archives and swell model simulation were provided by Larry Hsu (NRL).

One additional note: because of the potential for the Swell Model to underpredict energy in cases where the energy has not yet been generated in the Swell Model input file (the WAM restart file), we do not present skill metrics (e.g., root-mean-square error) in these cases.

Swell Model: Summary

These comparisons of WAM4 to the Navy Swell Model suggest that even with a first-order propagation scheme and coarse resolution, numerics and resolution are not a dominant source of error. This is despite the fact that in our comparison we use time periods, geographic locations, and fre-

quency ranges that are dominated by the type of wave for which one would tend to see the largest problems associated with poor numerics and coarse resolution (older swells).

This does not imply that first-order numerics applied at coarse resolution are accurate. It is more correct to say that the inaccuracies are significant but tend to be masked by spectral integration. (For example, error associated with diffusion will tend to alternate between positive and negative. Since these peaks and valleys tend to occur at different time/locations for different spectral components, integration of spectral components will usually lead to a cancellation of errors).

WAVEWATCH-III Hindcast Descriptions

Except for the Swell Model/WAM4 applications described above, the hindcasts shown in this report are limited to three hindcast cases, of approximately 1-month duration each. In some of these comparisons, we also include some WAM4 results. Most of the WAM4 results are from restart files (analyses only, archived by Larry Hsu, NRL) of the operational (NAVO) WAM4 (provided by James Dykes, NAVO). The NCEP-forced WAM4 simulations were run by Paul Wittmann (FNMOC), using data files provided by NCEP (July 2001 and January 2002 cases only). The Navy Swell Model was not applied in these three hindcasts. The July 2001 case would be an appropriate application of the Swell Model, since it is characterized by old swells. The other two cases, since they are characterized by younger swells, would not be appropriate (unless perhaps the buoys near Hawaii were included in the comparisons).

Although these are global applications, we compare only buoys in the Pacific Ocean. This is primarily due to swell propagation tendencies in the Pacific vs. the Atlantic.

January 2001

Our primary hindcast case for prediction of young swell is January 2001; it corresponds (to some degree) to the wind field accuracy check described in Section 3. We compare model output to NDBC buoy 46059, which is in deep water offshore of San Francisco. Most of the wave energy reaching this buoy during this period is from young swells (1-5 days old) generated in the North Pacific.

The hindcast period starts at 0000 UTC January 1 and ends 1800 UTC January 31. A ramp up time of 5 days was used in the January 2001 hindcasts (model output from the first 5 days is discarded in the root-mean-square error (RMSE) and bias calculations presented below. Of course, the ramp time is not necessary in cases where restart files from operational model runs were used, but it is included to be consistent with the hindcasts.

July 2001

July 2001 is the only one of the three hindcast cases that includes older (greater than 8 days) swells. It corresponds (to some degree) with the July 2001 investigation of wind field accuracy described in Section 3. As in the Swell Model applications presented above, low-frequency energy at the Pacific NDBC buoys during this time period is dominated by swells generated by strong wind events in the southern Pacific Ocean. We compare low-frequency wave heights at two locations: the Christmas Island buoy (51028) and buoy 46059 (again). When these swells reach buoy 51028, they tend to be of medium age (4-6 days old), but when they reach 46059, they are relatively old (greater than 8 days old).

The hindcast period starts at 0000 UTC July 1 and ends 1800 UTC July 31. A ramp time of 11 days is assumed in the July 2001 hindcasts.

January/February 2002

A second hindcast case was conducted, primarily as a check on repeatability of the other "young swells" hindcast. Here, instead of buoy 46059, low-frequency wave energy is compared at NDBC buoys 46006 (west of Northern California) and 46042 (just west of Monterey). Both buoys are in deep water.

The hindcast period starts at 0000 UTC January 1 and ends 2100 UTC February 8. A ramp time of 6 days is assumed in the January/February 2002 hindcasts.

Skill Metrics

To describe the success (or failure) of the various models in these three hindcasts, we use low-frequency wave height described in Section 1, with the wave heights being calculated from variance of wave spectra up to three different frequencies: 0.06, 0.08, and 0.10 Hz. To maintain legibility of this report, we present only the "up to 0.08 Hz results" in the main text; the 0.06 and 0.10 Hz results are shown in Appendix B.

Because of the number of comparisons made, we do not present all of them graphically. Instead, two skill metrics are tabulated: root-mean-square error and bias (mean error). A few graphical comparisons are made in each case. To isolate specific model characteristics, rather than listing all simulations for each hindcast in a single table, we present several comparisons each for the January 2001 and July 2001 hindcasts This leads to redundancy, since some simulations are listed multiple times, but (hopefully) this facilitates reading. In each case, simulations are ranked according to performance.

We choose to use RMS error rather than some variety of normalized error because we are particularly interested in the skill of models to predict stronger wave events rather than weighting weaker and smaller events more equally.

Numerical Scheme and Source/Sink Term: Sensitivity

The WvW3 code allows dual options for both numerical schemes:

- the first-order, upwind, explicit scheme, or
- the ULTIMATE QUICKEST (UQ) scheme and limiter and source/sink terms:
  - — the WAM Cycle 3 physics (input and dissipation of Komen et al. 1984) (KHH), or
  - — TC physics.

By applying hindcasts with different options, we can investigate the effect of numerical scheme and source/sink terms. Unfortunately, there is no "exact" Eulerian scheme (in the context of global hindcasting with a third generation wave model) or source/sink term, so this is more a test of sensitivity, with only hints with regard to accuracy. With regard to model numerics, the comparison of WvW3 with UQ numerics vs WvW3 with O(1) numerics is comparable to the comparison of WAM4 to the Navy Swell model. However, the former comparison is more limited, since (a) the UQ scheme is not exact, and (b) resolution is not varied in the WvW3 comparison. One could investigate resolution sensitivity by running WvW3 hindcasts at much higher resolution, but we did not do this.

The following figures and tables describe six cases: two forcing alternatives (NOGAPS and NCEP) and three hindcast/location combinations (January 2001 younger swells, July 2001 medium age swells, July 2001 older swells).

January 2001

Figure 19 shows an example graphic of the January 2001 hindcast case comparing WvW3 simulations, all with NCEP forcing, but with three different source/sink term combinations. Tables 3 and 4 show results for models with both forcings.

Here, the added diffusion of the first-order propagation scheme (vs the UQ scheme) is noticeable, but slight. All models are biased low. The difference between the TC physics and KHH is large, with KHH physics tending to underpredict energy more than other formulations. The difference between WAM4 physics and TC physics is significant. With NOGAPS forcing, WAM4 shows moderately better metrics than TC.

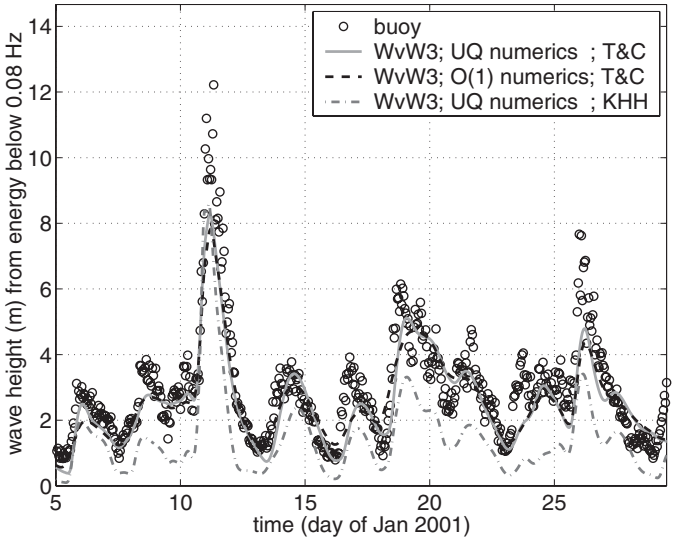

Fig. 19 — Comparison of three models vs buoy data. Low-frequency wave height is shown (energy up to 0.08 Hz). Location is NDBC buoy 46059 (offshore of San Francisco). Time period is January 2001. All three models are forced with NCEP winds. Plot indicates relative impact of physics and numerics.

Table 3 – Error measures based on energy up to 0.08 Hz for January 2001 hindcast at location of NDBC buoy 46059 (west of San Francisco). Hindcasts with NOGAPS forcing are shown. Models are ranked according to skill for this particular case. (WAM4 result provided by Larry Hsu, NRL.)

January 2001. NOGAPS forcing. Buoy 46059. H_{m0} based on frequencies up to 0.08 Hz				
Model Platform	Numerics	Physics	Bias (m)	RMSE (m)
WAM4	O(1)	WAM4	–0.99	1.38
WvW3	UQ	TC	–1.29	1.81
WvW3	O(1)	TC	–1.33	1.89
WvW3	O(1)	KHH	–2.11	2.49
WvW3	UQ	KHH	–2.16	2.51

Table 4 – Error measures based on energy up to 0.08 Hz for January 2001 hindcast at location of NDBC buoy 46059 (west of San Francisco). Hindcasts with NCEP forcing are shown. Models are ranked according to skill for this particular case.

January 2001. NCEP forcing. Buoy 46059. WvW3 model. H_{m0} based on energy up to 0.08 Hz		
Numerics	Physics	Bias (m)
O(1)	TC	–0.34
UQ	TC	–0.38
O(1)	KHH	–1.41
UQ	KHH	–1.44
Numerics	Physics	RMSE (m)
UQ	TC	0.82
O(1)	TC	0.84
O(1)	KHH	1.65
UQ	KHH	1.66

July 2001

In the July 2001 cases (Fig. 20, Tables 5-8), diffusion is more significant than in the January 2001 case, but it still has less impact, on average, than physical formulation (and strangely enough, the diffusion is more apparent in the medium-age swells (51028) than in the old swells (46059)).

At the 51028 location (younger swells), WAM4 is only slightly more energetic than the TC-based models. But interestingly, at the 46059 location (older swells), these same swells are much more energetic in the WAM4-based model than in the TC-based model. Presumably, this is due to the negative S_{in} term in TC physics, which does not exist in WAM4 physics (alternately, dissipation of swells by the S_{ds} term may be stronger in TC physics than WAM4 physics, but if this difference exists, we are not aware of it). According to these comparisons, the level of attenuation of swells by S_{ds} and S_{in} appears to be more skillful in the TC-based models (WAM4 physics do not attenuate swell enough). Tolman (2002a) comes to a similar conclusion, and suggests that WAM4 might benefit from implementation of a negative wind input term. We note that attenuation of swells, over long distances such as these, can be very sensitive to the handling of the high-frequency tail. Based on personal experience, and discussions with Peter Janssen (ECMWF), this is particularly true with WAM3 physics (used by the SWAN model, for example).

If swell attenuation is real and significant, this could impact the Navy Swell Model, which presently assumes zero dissipation of swell. One might speculate that problems with under-dissipation in the Swell Model have never been noticed, because of persistent under-generation in the driver model (WAM4). To determine this, further study is required.

Even with the higher-order propagation scheme, the swell events at buoy 46059 appear to be overly smoothed relative to the measurements. This smoothing may be due to incorrect frequency distribution (too broad), which in turn may be due to inaccuracies associated with the DIA.

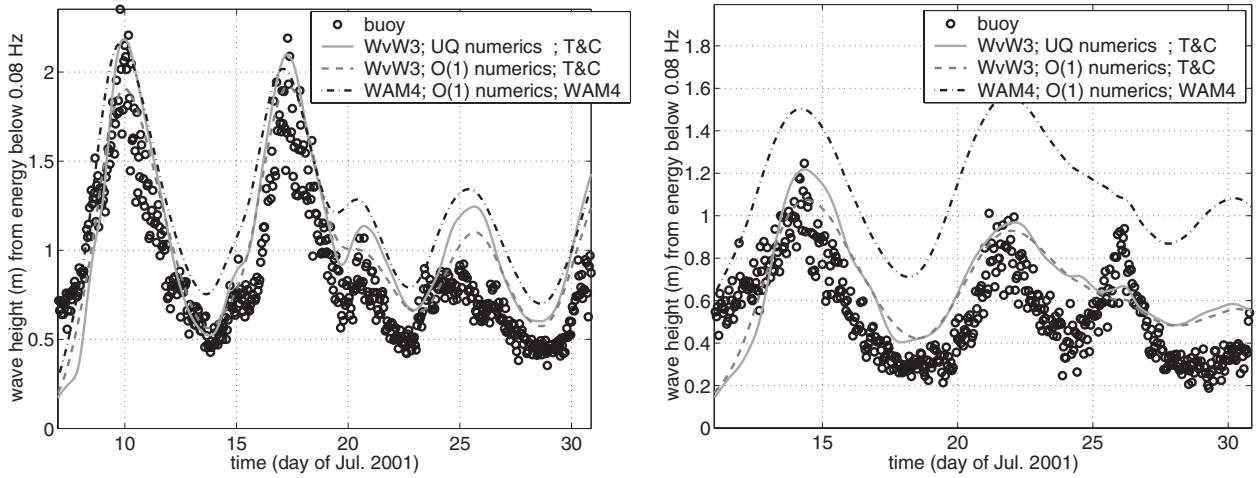

(a) Location is NDBC buoy 51028 (Christmas Island buoy)

(b) Location is NDBC buoy 46059 (offshore of San Francisco)

Fig. 20 — Comparison of three models vs buoy data. Low-frequency wave height is shown (energy up to 0.08 Hz). Time period is July 2001. All three models are forced with NCEP winds. Plot indicates relative impact of physics and numerics. WAM4 simulation created by Paul Wittmann (FNMOC).

Table 5 – Error measures based on energy up to 0.08 Hz for July 2001 hindcast at location of NDBC buoy 51028 (Christmas Island). Hindcasts with NOGAPS forcing are shown. Models are ranked according to skill for this particular case. (WAM4 result provided by Larry Hsu, NRL.)

July 2001. NOGAPS forcing. Buoy 51028. H_{m0} based on energy up to 0.08 Hz			
Model Platform	Numerics	Physics	Bias (m)
WAM4	O(1)	WAM4	–0.04
WvW3	UQ	TC	–0.13
WvW3	O(1)	TC	–0.17
Model Platform	Numerics	Physics	RMSE (m)
WvW3	UQ	TC	0.21
WAM4	O(1)	WAM4	0.24
WvW3	O(1)	TC	0.25

Table 6 – Error measures based on energy up to 0.08 Hz for July 2001 hindcast at location of NDBC buoy 51028 (Christmas Island). Hindcasts with NCEP forcing are shown. Models are ranked according to skill for this particular case. (WAM4 result provided by Paul Wittmann, FNMOC.)

July 2001. NCEP forcing. Buoy 51028. H_{m0} based on energy up to 0.08 Hz				
Model Platform	Numerics	Physics	Bias (m)	RMSE (m)
WvW3	O(1)	TC	0.20	0.24
WvW3	UQ	TC	0.25	0.30
WAM4	O(1)	WAM4	0.37	0.40

Table 7 – Error measures based on energy up to 0.08 Hz for July 2001 hindcast at location of NDBC buoy 46059 (west of San Francisco). Hindcasts with NOGAPS forcing are shown. Models are ranked according to skill for this particular case. (WAM4 result provided by Larry Hsu, NRL.)

July 2001. NOGAPS forcing. Buoy 46059. H_{m0} based on energy up to 0.08 Hz				
Model Platform	Numerics	Physics	Bias (m)	RMSE (m)
WvW3	UQ	TC	-0.14	0.26
WvW3	O(1)	TC	-0.15	0.26
WAM4	O(1)	WAM4	0.26	0.30

Table 8 – Error measures based on energy up to 0.08 Hz for July 2001 hindcast at location of NDBC buoy 46059 (west of San Francisco). Hindcasts with NCEP forcing are shown. Models are ranked according to skill for this particular case. (WAM4 result provided by Paul Wittmann, FNMOC.)

July 2001. NCEP forcing. Buoy 46059. H_{m0} based on energy up to 0.08 Hz				
Model Platform	Numerics	Physics	Bias (m)	RMSE (m)
WvW3	O(1)	TC	0.12	0.21
WvW3	UQ	TC	0.13	0.23
WAM4	O(1)	WAM4	0.58	0.61

Impact of Forcing: Degree of Data Usage in Blended NOGAPS/QuikSCAT Fields

The January 2001 and July 2001 hindcasts were conducted with varying degrees of data-usage in forcing:

- NOGAPS only. (This case is presented in Section 5 also.)
- L2B, W3: The JPL L2B QuikSCAT data (described in Section 1) are used in instances where data are available within three hours (before or after) the time of the snapshot (as described in Section 4).
- L2B, W6: The JPL L2B data are used in instances where data are available within 6 hours (before or after) the time of the snapshot (as described in Section 4).
- L3, W∞: The JPL L3 data are used at all data points.

Figure 14 shows example wind field maps created with varying degrees of data usage (L3, W∞ is not shown; L3, W12 is shown instead.). Tables 9-11 compare results from application to the two hindcasts. The use of data is very effective at removing the negative bias associated with the NOGAPS forcing. However, in the case of the July 2001 swells, there is some overshoot (i.e., use of data leads to overprediction).

Since none of these four forcing fields provides consistently better error measures in these three cases, we must choose a "degree of data usage" based on other considerations. As mentioned in Section 4, the choice of "degree of data usage" is somewhat subjective, dependent on the level of bias in the atmospheric model. In our case, we would clearly benefit from making the "degree of data usage" such that it varies with season and geographic location, according to the level of bias. This is a planned improvement. We choose the L2B, W6 criterion for data usage for use in later comparisons, since that provides reasonably good coverage (by QuikSCAT) of the ocean's surface ("within 3 hours" leaves rather large gaps, and "within 12 hours" is probably too aggressive).

Table 9 – Error measures based on energy up to 0.08 Hz for January 2001 hindcast at location of NDBC buoy 46059 (west of San Francisco). WvW3 hindcasts (default physics (TC) and numerics (UQ)) with varying degrees of data usage in forcing are shown (NOGAPS background). Models are ranked according to skill for this particular case.

January 2001. WvW3 model. Buoy 46059. H_{m0} based on energy up to 0.08 Hz		
Forcing	Bias (m)	RMSE (m)
NOGAPS+QuikSCAT (L2B, W6)	0.05	0.72
L3 (W∞)	0.25	0.78
NOGAPS+QuikSCAT (L2B, W3)	–0.64	1.02
NOGAPS	–1.29	1.81

Table 10 – Error measures based on energy up to 0.08 Hz for July 2001 hindcast at location of NDBC buoy 51028 (Christmas Island). WvW3 hindcasts (default physics (TC) and numerics (UQ)) with varying degrees of data usage in forcing are shown (NOGAPS background). Models are ranked according to skill for this particular case.

July 2001. WvW3 model. Buoy 51028. H_{m0} based on energy up to 0.08 Hz		
Forcing	Bias (m)	RMSE (m)
NOGAPS	–0.13	0.21
NOGAPS+QuikSCAT (L2B, W3)	0.17	0.23
NOGAPS+QuikSCAT (L2B, W6)	0.43	0.48
L3 (W∞)	0.58	0.61

Table 11 – Error measures based on energy up to 0.08 Hz for July 2001 hindcast at location of NDBC buoy 46059 (west of San Francisco). WvW3 hindcasts (default physics (TC) and numerics (UQ)) with varying degrees of data usage in forcing are shown (NOGAPS background). Models are ranked according to skill for this particular case.

July 2001. WvW3 model. Buoy 46059. H_{m0} based on energy up to 0.08 Hz		
Forcing	Bias (m)	RMSE (m)
NOGAPS+QuikSCAT (L2B, W3)	0.08	0.22
NOGAPS	–0.14	0.26
NOGAPS+QuikSCAT (L2B, W6)	0.29	0.35
L3 (W∞)	0.39	0.43

In these comparisons, we hold constant the wave model itself (we use the WvW3 model with default physics (TC) and numerics (UQ)).

Impact of Forcing: Atmospheric Model Analyses vs Blended NOGAPS/QuikSCAT Fields

Here, we hold constant the wave model itself (some comparisons use WvW3 with default numerics and physics, and other comparisons use WAM4), and we vary the forcing used, with the forcing techniques being:

- NOGAPS analyses
- NCEP analyses
- QuikSCAT data blended with NOGAPS analyses (L2B, W6)
- COAMPS ("East Pacific" domain) blended with NOGAPS analyses.

COAMPS (Coupled Ocean/Atmospheric Mesoscale Prediction System) is the regional model currently used by the operational Navy (FNMOC) (Hodur 1997, Hodur et al. 2002). Since it is higher resolution than NOGAPS, it is expected to be more skillful. We investigate the impact of augmenting the forcing of the global wave model with this regional atmospheric model (and in the process, hopefully removing some of the bias in the NOGAPS forcing). Other COAMPS models exist, but only the East Pacific model is used here. COAMPS and NOGAPS are blended simply by replacing NOGAPS with COAMPS at appropriate locations in the NOGAPS ($1° \times 1°$) grid, with no smoothing of the transition (since the wave model does not require it). This blended field is applied only to the January 2001 case. Figure 21 shows example NOGAPS wind fields, with and without the COAMPS augmentation.

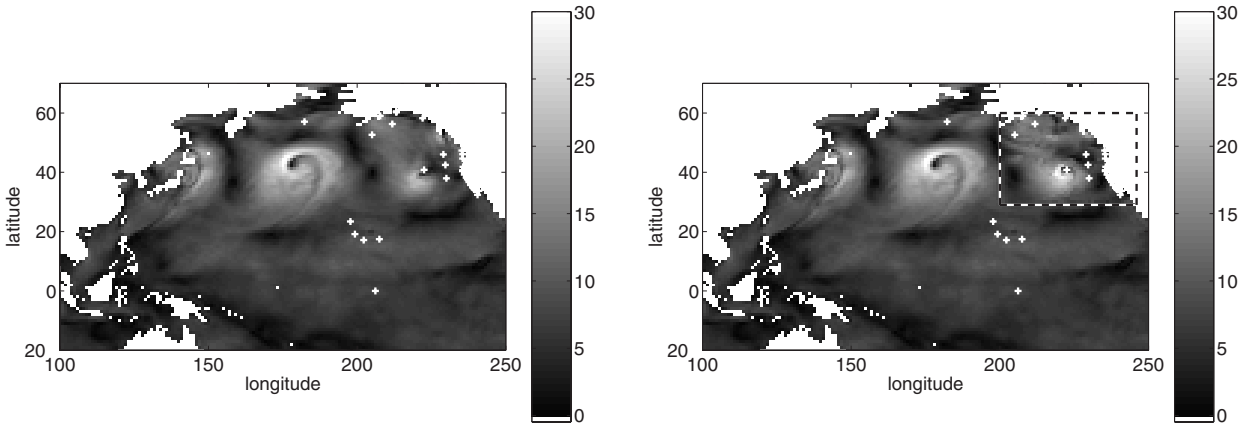

(a) NOGAPS field

(b) Blending of NOGAPS and EPAC COAMPS (regional) model

Fig. 21 — Portion of wind field used to force global model. Time is 0600 UTC January 10 2001. COAMPS domain is indicated by dashed rectangle. Locations of NDBC buoys are indicated with crosses.

Note that again, this is a sensitivity test. It is not a direct check on wind field accuracy. However, we can probably presume that if we get consistently better results with a given wind product, then it is a better product. The assumption here is that the conclusions are not skewed in favor of one forcing technique vs another due to inaccuracies in the wave model itself.

January 2001

Figure 22 and Table 12 present comparisons for January 2001. Here, the blended QuikSCAT/ NOGAPS result compares very favorably to the operational products: the negative bias is eliminated with very little "overshoot". The COAMPS augmentation is also very effective at reducing the negative bias, but as would be expected, is only beneficial to swells that were generated within the COAMPS grid. For example, the January 12 swell event was generated within the COAMPS grid region, whereas the January 19 event was not. The proximity of the January 12 wind event also explains the large magnitude of the event (the magnitude of the spectral density has not yet been reduced by dispersion).

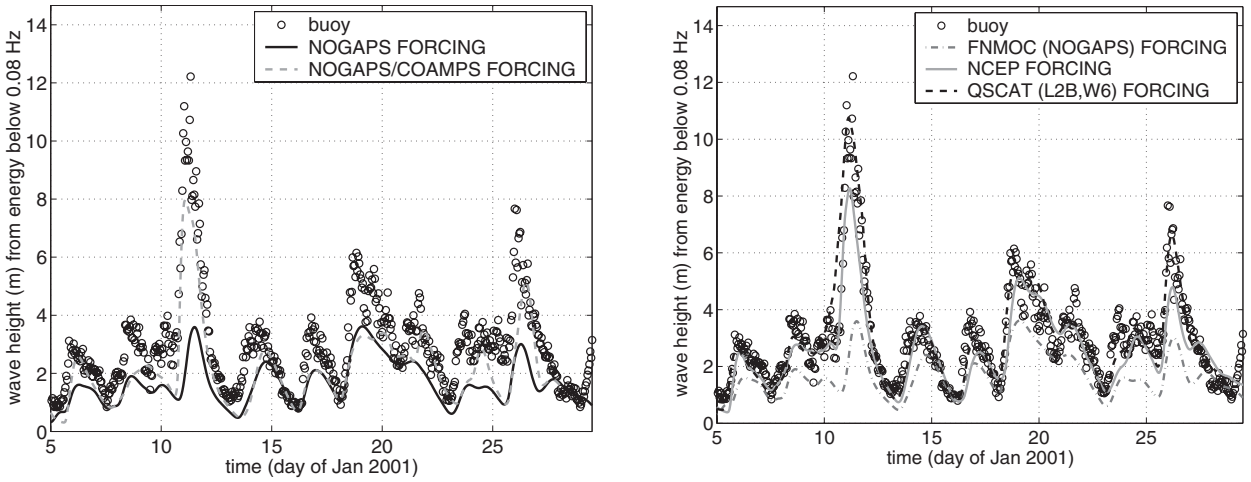

Fig. 22 — Comparison of models vs buoy data. Low-frequency wave height is shown (energy up to 0.08 Hz). Location is NDBC buoy 46059 (offshore of San Francisco). Time period is January 2001. All models are WvW3 with default physics and numerics.(a) Plot indicates the impact of supplementing NOGAPS wind forcing with regional atmospheric (COAMPS) model, in forcing the global wave model (i.e., the two forcing techniques differ only in COAMPS region indicated in Fig. 21.); (b) Plot compares wave model results with three forcing techniques that differ globally.

Table 12 – Error measures based on energy up to 0.08 Hz for January 2001 hindcast at location of NDBC buoy 46059 (west of San Francisco). WvW3 hindcasts (default physics (TC) and numerics (UQ)) with different forcing fields are shown. Models are ranked according to skill for this particular case.

January 2001. WvW3 model (default physics/numerics). Buoy 46059. H_{m0} based on energy up to 0.08 Hz		
Forcing	Bias (m)	RMSE (m)
NOGAPS+QuikSCAT (L2B, W6)	0.05	0.72
NCEP	–0.38	0.82
NOGAPS/COAMPS	–0.86	1.21
NOGAPS	–1.29	1.81

July 2001

Figure 23 and Tables 13-16 compare the July 2001 hindcasts. The tabulated results for buoy 51028 indicate that the WvW3 model performs better with NOGAPS forcing than with NCEP or blended forcing. This is rather peculiar since in Section 3 we demonstrated that the NCEP winds appear to be more accurate than the NOGAPS winds in the southern Pacific Ocean during July 2001.

Because of this peculiarity, we investigate this comparison in greater detail: see Figs. 24-26. Although the NOGAPS-forced model has the most favorable metrics in this case, it does have severe problems: the mean periods and total energy are both biased low, suggesting that the winds at the generation time/location are too weak. The models forced by the blended (NOGAPS/QuikSCAT) wind fields and NCEP wind fields tend to overpredict total energy (H_{m0} bias of 0.43 and 0.25 m, respectively) but are much more successful than the NOGAPS-forced model at predicting the position of spectra (mean period). One possible explanation is that the wave model is accurately predicting the spectral distribution at the source (we did not verify that this is the case), but somehow the spectral density is not being diminished properly, either by dispersion (modeled directional distribution is incorrect) or by attenuation (swell is attenuated in nature more than in the model). Neither explanation is very satisfying, since it leaves the question of why we do not see the same trend in the January 2001 case. The typical swell ages for buoy 51028 during July are not too dissimilar from the those for buoy 46059 during January (typically 4-6 day old swell for the former and 1-5 day old swell for the latter). However, the July 51028 swells tend to be much lower (even at their origin) and less frequent than the January 46059 swells. Perhaps this difference in wave climate explains the discrepancy.

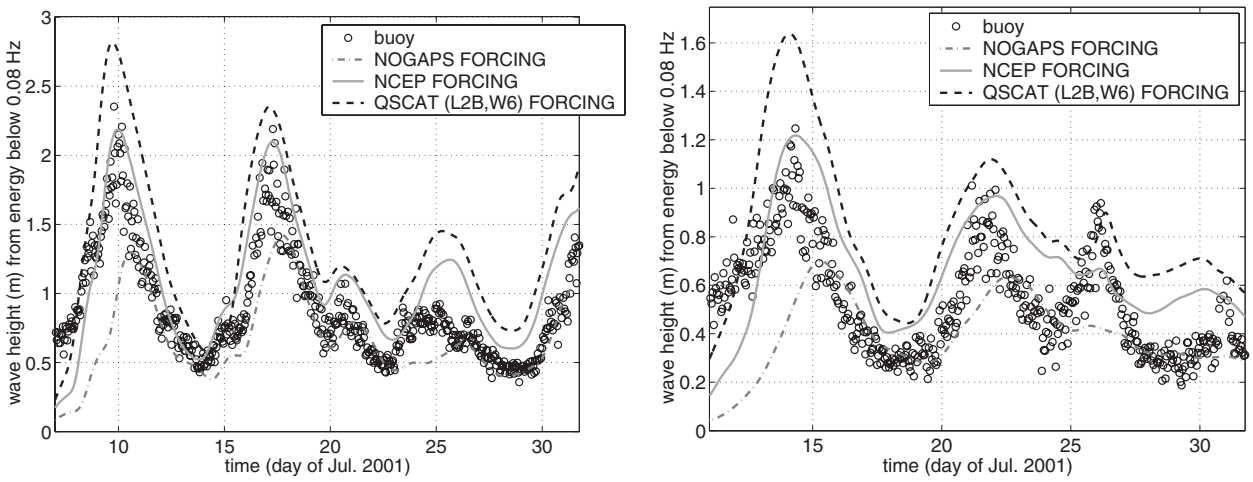

(a) Location is NDBC buoy 51028 (Christmas Island buoy)

(b) Location is NDBC buoy 46059 (offshore of San Francisco)

Fig. 23 — Comparison of three models vs buoy data. Low-frequency wave height is shown (energy up to 0.08 Hz). Time period is July 2001. All three models are WvW3 with default physics and numerics. Plot indicates impact of three different forcing techniques.

Table 13 – Error measures based on energy up to 0.08 Hz for July 2001 hindcast at location of NDBC buoy 51028 (Christmas Island). WvW3 hindcasts (default physics (TC) and numerics (UQ)) with different forcing fields are shown. Models are ranked according to skill for this particular case.

July 2001. WvW3 model (default physics/numerics). Buoy 51028. H_{m0} based on energy up to 0.08 Hz		
Forcing	Bias (m)	RMSE (m)
NOGAPS	–0.13	0.21
NCEP	0.25	0.30
NOGAPS+QuikSCAT (L2B, W6)	0.43	0.48

Table 14 – Error measures based on energy up to 0.08 Hz for July 2001 hindcast at location of NDBC buoy 51028 (Christmas Island). WAM4 hindcasts with different forcing fields are shown. Models are ranked according to skill for this particular case. (WAM4 results were provided by Larry Hsu, NRL and Paul Wittmann, FNMOC.)

July 2001. WAM4 model. Buoy 51028. H_{m0} based on energy up to 0.08 Hz		
Forcing	Bias (m)	RMSE (m)
NOGAPS	–0.04	0.24
NCEP	0.37	0.40

Table 15 – Error measures based on energy up to 0.08 Hz for July 2001 hindcast at location of NDBC buoy 46059 (west of San Francisco). WvW3 hindcasts (default physics (TC) and numerics (UQ)) with different forcing fields are shown. Models are ranked according to skill for this particular case.

July 2001. WvW3 model (default physics/numerics). Buoy 46059. H_{m0} based on energy up to 0.08 Hz		
Forcing	Bias (m)	RMSE (m)
NCEP	0.13	0.23
NOGAPS	–0.14	0.26
NOGAPS+QuikSCAT (L2B, W6)	0.29	0.35

Table 16 – Error measures based on energy up to 0.08 Hz for July 2001 hindcast at location of NDBC buoy 46059 (west of San Francisco). WAM4 hindcasts with different forcing fields are shown. Models are ranked according to skill for this particular case. (WAM4 results were provided by Larry Hsu (NRL) and Paul Wittmann (FNMOC).)

July 2001. WAM4 model. Buoy 46059. H_{m0} based on energy up to 0.08 Hz		
Forcing	Bias (m)	RMSE (m)
NOGAPS	0.26	0.30
NCEP	0.58	0.61

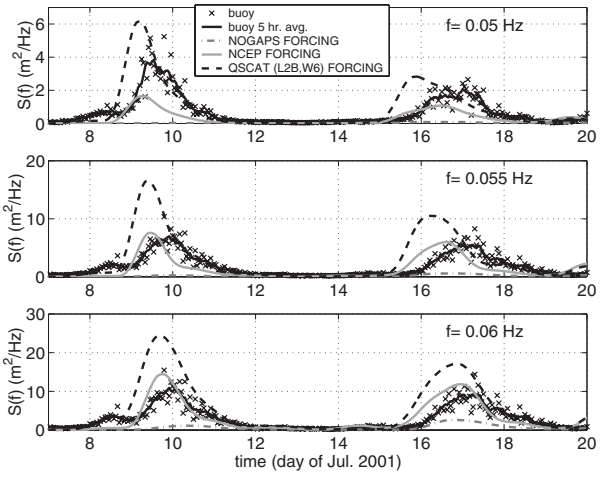

(a) 0.05, 0.055, 0.06 Hz

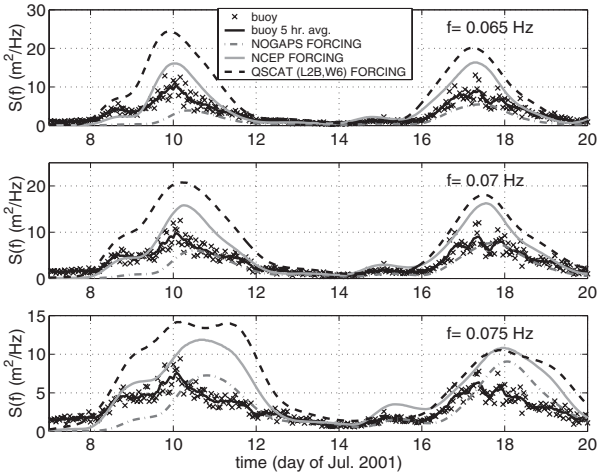

(b) 0.065, 0.07, 0.075 Hz

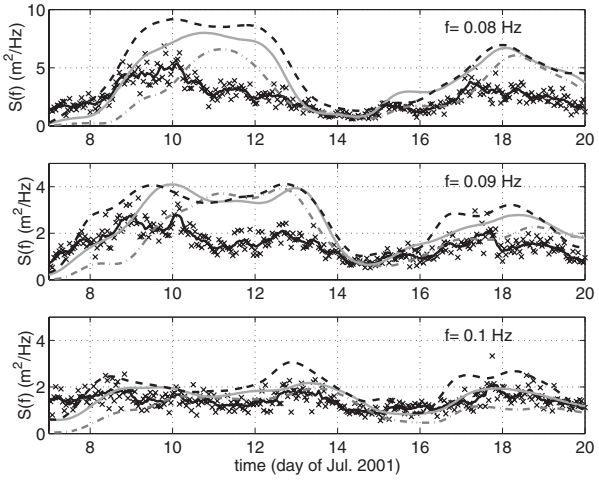

(c) 0.08, 0.09, 0.10 Hz

Fig. 24 — As Fig. 23(a), except spectral density is shown, rather than wave height. Instantaneous (reported hourly) buoy spectral density is shown with x's. A 5-h moving average of buoy data is also shown to reduce apparent nonstationarity caused by random error in measurements.

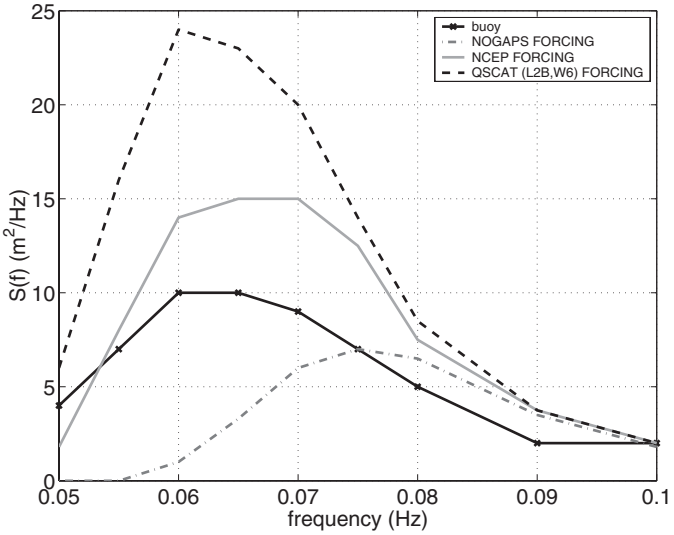

Fig. 25 — As Fig. 24, except one-dimensional spectra from the buoy and three models are shown. These are the (approximate, average) "representative" spectra associated with July 9, 2001. This is shown to provide a visual aid for interpreting the general trend in bias in Fig. 24.

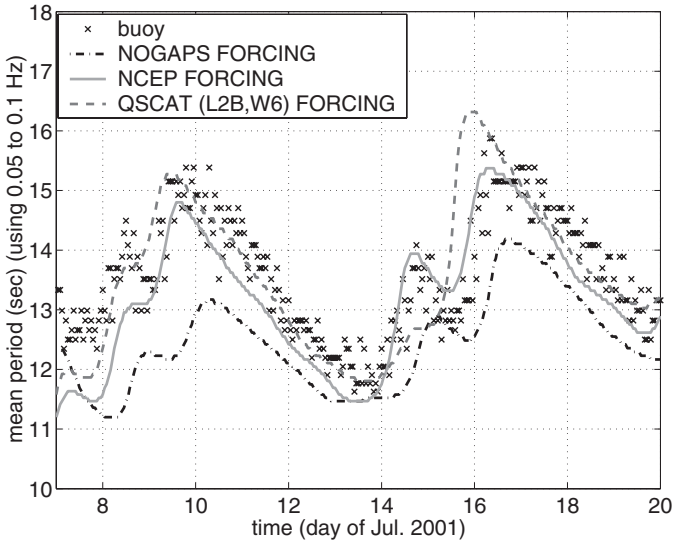

Fig. 26 — As Fig. 23, except mean period is shown. Mean period is calculated as the inverse of the centroid of the frequency spectrum over the interval 0.05 to 0.10 Hz

Repeatability Check: January 2002

Because the results of the January 2001 were rather inconsistent with those of July 2001, we performed at repeatability check for the January swell hindcasting: January 2002. We test not only the repeatability in terms of general location and season (northeast Pacific, winter time), but also in terms of specific location and instrument type. (We use 46006, which is northwest of 46059; and 46042, which is southeast of 46059. Buoy 46042 is a 3-m discus buoy, whereas buoys 46059 and 46006 are 6-m Nomad buoys.) Results are shown in Tables 17 and 18 and Fig. 27. In both cases, the WvW3 models forced by either NCEP winds or blended (NOGAPS+QuikSCAT) winds perform very well. In

Table 17 – Error measures based on energy up to 0.08 Hz for January 2002 hindcast at location of NDBC buoy 46006 (west of Northern California). Models are ranked according to skill for this particular case. (WAM4 results were provided by Larry Hsu (NRL) and Paul Wittmann (FNMOC).)

January 2002. Buoy 46006. H_{m0} based on energy up to 0.08 Hz			
Model Platform (default physics/numerics)	Forcing	Bias (m)	RMSE (m)
WvW3	NCEP	0.01	0.52
WvW3	NOGAPS+QuikSCAT (L2B, W6)	0.13	0.54
WAM4	NCEP	–0.13	0.59
WvW3	NOGAPS	–0.65	0.95
WAM4	NOGAPS	–0.69	1.00

Table 18 – Error measures based on energy up to 0.08 Hz for January 2002 hindcast at location of NDBC buoy 46042 (west of Monterey, California). Models are ranked according to skill for this particular case. (WAM4 results were provided by Larry Hsu (NRL) and Paul Wittmann (FNMOC).)

January 2002. Buoy 46042. H_{m0} based on energy up to 0.08 Hz		
Model Platform (default physics/numerics)	Forcing	Bias (m)
WvW3	NCEP	–0.01
WvW3	NOGAPS+QuikSCAT (L2B, W6)	0.05
WAM4	NCEP	–0.12
WvW3	NOGAPS	–0.48
WAM4	NOGAPS	–0.52
Model Platform (default physics/numerics)	Forcing	RMSE (m)
WvW3	NOGAPS+QuikSCAT (L2B, W6)	0.32
WAM4	NCEP	0.41
WvW3	NCEP	0.42
WvW3	NOGAPS	0.68
WAM4	NOGAPS	0.69

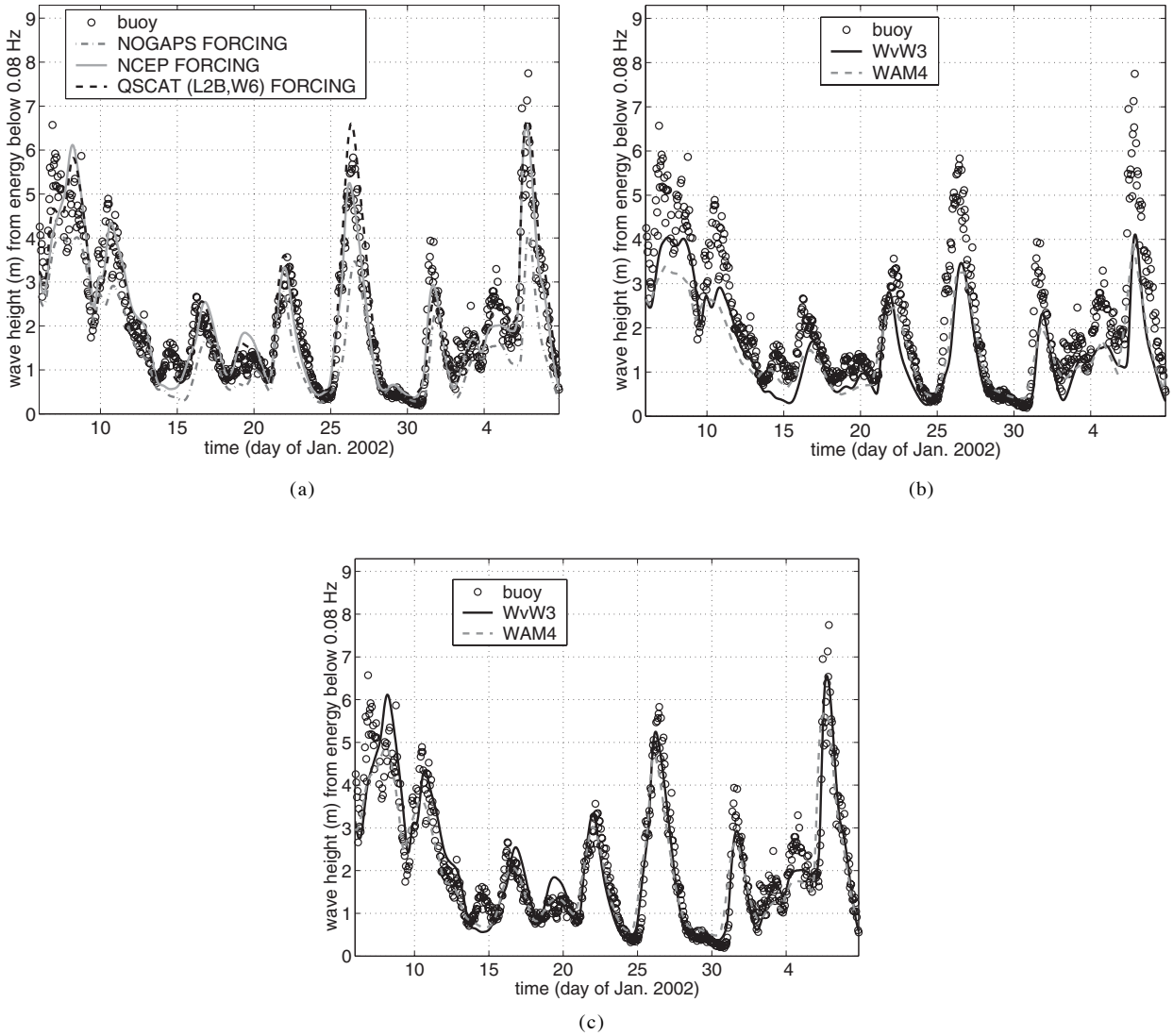

Fig. 27 — Comparison of models vs buoy data for January 2002 hindcast, at location of NDBC buoy 46006 (offshore of northern California). Low-frequency wave height is shown (energy up to 0.08 Hz). (a) Comparison of results with three different forcing techniques. All three models are WvW3 with default physics and numerics. (b) Comparison of model results with different physics and numerics. Both models are forced with NOGAPS. (c) As 27(b), except that both models are forced with NCEP analyses.

mid-January 2002, NCEP began to assimilate QuikSCAT data in their operational product (Hendrik Tolman, personal communication). It is remarkable that the NCEP-forced wave model and the blended (QuikSCAT+NOGAPS) field-forced wave model are nearly identical for the January 8 swell event (which is prior to the beginning of NCEP's assimilation). When provided the same forcing, the similarity of the two models (WvW3 and WAM4), each with different physics and numerics, is also remarkable, and serves as a compelling argument that (at least in this case), wind forcing is the dominant source of error. The low-frequency wave events have a tendency to peak sooner in the WAM4 model, but higher in the WvW3 model. This is consistent with WAM4/WvW3 comparisons made by Paul Wittmann (FNMOC, personal communication), and may be explained by the behavior of the two models in the canonical comparisons (Section 3), where WAM4 shows stronger growth in the short fetch/duration regimes, and WvW3 exceeding WAM4 in the longer fetch/duration regimes.

The NOGAPS-forced models have large negative bias, whereas the WvW3 model forced by NCEP winds has only a very small bias.

We also performed "sanity checks" with this case by comparing

- the NAVO WAM4 run in operational mode, using NOGAPS forcing vs the WAM4 model run at FNMOC in hindcast mode with archived NOGAPS forcing (a sanity check on other WAM4 hindcasts run at FNMOC), and

- the FNMOC WvW3 model run in operational mode, using NOGAPS forcing vs the NRL WvW3 model run in hindcast mode with archived NOGAPS forcing. The WvW3 restart files are sent (by Paul Wittmann) from FNMOC to NRL (the author), where they are archived.

In both cases, the discrepancies were very small and could be attributed to known (minor) differences between the models. For example the FNMOC WvW3 model accounts for air-sea temperature differences, whereas the NRL WvW3 model does not. Also, the NRL WvW3 models interpolated spectra to the buoy locations, whereas the other models used the nearest computational node on the $1° \times 1°$ grid.

General Observations Regarding the Three Hindcasts

In general, the results from the January hindcasts were intuitive, while the July 2001 hindcasts were sometimes puzzling.

With regard to differences between NOGAPS-forced models and NCEP-forced models, in general, the difference is much larger in the two January cases than in the one July case. This is consistent with the direct check on forcing accuracy using QuikSCAT measurements (Section 3), which showed that the skill difference of NCEP winds vs NOGAPS winds is greater in the north Pacific winter than in the southern Pacific Ocean winter (for the regions and months that we used).

The models forced by the blended (NOGAPS/QuikSCAT) wind fields are consistently more energetic than the other models, suggesting that the QuikSCAT winds tend to be stronger than the model winds. This is consistent with the wind field validation in Section 3, in which (for January 2001 and July 2001) both NOGAPS and NCEP winds appeared to be biased low at higher wind speeds, if the QuikSCAT data are taken as ground truth.

The first-order error source appears to be the wind forcing, while model physics appear to be of second order. Although the impact of physics tends to be significant, it is difficult to make a judgment regarding the skill of WAM4 physics vs WvW3 (TC) physics. This is especially true with regard to the generation stage, where comparisons (of younger swells to buoy data) were ambiguous. The physics of swell dissipation does, however, appear to be better represented in WvW3 than in WAM4 (swell may not be dissipated enough in WAM4).

The dominant impact of wind forcing is consistent with the conclusions of Cardone et al. (1996). This study dealt with several wave models, including WAM4. Their analysis is in terms of total wave height (rather than low-frequency wave height), but since they focus on extreme events which are, by definition, dominated by low-frequency energy, the study is pertinent to low-frequency energy. They find that, given accurate forcing, wave model bias is very small, and that in operational nowcast/forecast systems, wind forcing is the dominant source of error.

The hindcasts lead us to believe that propagation numerics tend to be less important than either forcing or physics; one might call it "third order." (This is not to be confused the order of the truncation error of the propagation scheme. In other words, the truncation error of the WAM4 propagation scheme is first order, but this does not appear to translate into a first-order component of the total "error budget" of the wave model.) This conclusion is consistent with the more precise check on numerics (using WAM4/Swell Model comparisons) presented in Section 3. The added accuracy of the higher order propagation numerics of WvW3 (vs the much less accurate first-order propagation numerics) do not appear to translate into significant added skill, even if we consider comparisons that would tend to favor a model with accurate numerics (e.g., skill at capturing peaks and valleys in a time series of low-frequency wave energy). The situation can be generally described as one in which a third-order error (numerics) does not have a consistent impact on model skill; it neither consistently counteracts nor consistently reinforces the first-order error (wind forcing). Note however, that there are advantages to higher order numerics that do not necessarily manifest in error statistics such as these. Namely, a model with higher order numerics will produce images of geographic distributions of swell fields that are much more realistic in appearance than would be produced with first-order numerics.

6. DISCUSSION

Quality of Data-derived Wind Fields

The level of improvement seen in some of our hindcasts by our data usage method suggests that this can be an effective means of reducing problems associated with bias in wind forcing. In our July 2001 case, there is some overshoot (data usage leads to too much wave energy). This may be due to shortcomings in the physical formulations or it may be an indication that we should use a more sophisticated technique of creating snapshot wind fields. We have identified possible methods for improving our technique and plan to implement them during FY03.

Subjectivity

Subjectivity is a recurring theme in this study. The definition of a "good" atmospheric model is subjective. To accurately predict low-frequency wave energy, we require accurate predictions of high wind speed events at the surface. Another application might require something completely different. To provide an example, the Emanuel cumulus parameterization scheme was implemented in NOGAPS (Hogan et al. 1999) and became operational in 2000. This improved precipitation and hurricane track forecasts, but unfortunately decreased surface wind predictions (Teixeira and Hogan 2001), which obviously can have a negative impact on the wave models.

Similarly, the definition of a "good" data-derived wind field is subjective. As mentioned earlier, it is not essential for a wave model that a forcing field be smooth, and wind curl is not directly relevant. Capturing the intensity and duration of strong wind events is important. An example: our comparison of FSU COAPS suggests that the fields might be smoothed too much for our application (peaks of events appear to be reduced too much in the time series). However, informal communications with other researchers indicate that, for their applications, these wind fields are not smoothed enough! And, we can probably safely presume that the creators of these wind fields (FSU) feel that the level of smoothing is quite ideal.

Recommendations

Potential Use for Data-derived Wind Fields by the Operational Navy

It is possible to take advantage of the fact that swell is always generated by wind analyses (never by wind forecast). Wind fields could be derived from measurements operationally, and even though the wind fields may not be available until, say 9 hours after the time of the measurements, that wind field could still be used in a swell forecast. There is already a mechanism in place for this at FNMOC: the "post-time analysis," by which the analysis winds are revised several hours after the initial analyses are made available. The NAVDAS (discussed in Section 4) may be providing such a wind field product some time in the future. In the meantime, the field-generation software described in this study (or, more likely, some more sophisticated evolution thereof) could be used as an interim solution (and would also provide a benchmark against which the NAVDAS product could be compared if/when it becomes available).

The other operational centers are already doing this sort of post-time ingesting of satellite data (Hendrik Tolman (NCEP), Peter Janssen (ECMWF), informal communication). But it is apparent that whatever use the NOGAPS model is making of satellite data (via its assimilation scheme), it is not enough to remove the large and apparently consistent negative bias at high winds speeds. It is clear that the skill of swell nowcasts and forecasts by the Navy wave models (FNMOC WvW3 and NAVO WAM4) would benefit greatly if more use were made of satellite data.

Source/Sink Term Development

Since alternative hindcast wind fields are available, the apparent bias with NOGAPS will not prevent or delay development of the source/sink terms used in the Navy's global models.

It is believed by many in the wave-modeling field that the greatest impediment to further development of source/sink terms is the inaccuracy of the DIA used operationally. We have not seen incontrovertible evidence that this is the case, but there are convincing arguments in this regard. Certainly DIA produces a markedly different S_{nl} solution than a more rigorous solver. Unfortunately, expense of these rigorous solvers limits their utility. Exercises in tuning S_{in} or S_{dis} with such a solver can provide considerable insight, but the resulting S_{in} or S_{dis} formulations will likely perform poorly when applied at global scale with the DIA solver.

Therefore, the development of a fast, accurate nonlinear solver should be a priority. Even if the accurate solver does not improve overall model skill as much as the community hopes, it will at least eliminate speculation that DIA is the cause of various problems, making it easier to find the true problem in each case. It is the author's opinion that there probably is significant error—which may or may not be apparent in comparisons herein—associated with the DIA. For example, the DIA is known to be too broad in frequency space, resulting in too much transfer to lower frequencies (e.g., Hasselmann et al. 1985, also confirmed in independent simulations by the author). We do not see a consistent overprediction of low-frequency energy in our hindcasts here (or operational output), which may suggest another situation of errors canceling.

The best approach to improvement of S_{in} and S_{dis} is a question that is rife with controversy at present. With regard to S_{in}, open issues are the directional distribution of the term, the wind speed scaling law (e.g., U_*, U_{10}, or $U_{\lambda L}$, where L is the wavelength and λ is some constant) and the physical argument for wind-to-waves momentum transfer. With regard to S_{dis}, careful empiricism appears to be the only feasible approach. The TC formulations, with their flexibility in tuning, may be the best foundation

for future development. In the applications presented here, both WAM4 and TC physics already appear to be doing quite well at predicting wave growth when forced with accurate winds, so necessary refinement may be modest in nature.

One goal that should be kept in mind is the necessity of a source/sink term package that tunes "universally," such that tuning to one scale does not degrade performance at another scale. This type of problem is discussed in Tolman (2002a).

For the author, perhaps the most surprising result of this study is the difference in swell attenuation (WAM4 physics vs TC physics) demonstrated in the July 2001 hindcast. The result tentatively suggests that WAM4 physics do not attenuate swell enough (similar to the suggestion of Tolman 2002a). This justifies further investigation (and perhaps refinement of WAM4 physics).

Numerics and Resolution

In the WvW3 model, the problem with coarse geographic resolution leading to inadequate blocking by islands will be addressed in the next version of the model using approximate methods (Tolman 2002b). Propagation scheme error has been improved via the UQ scheme, and the Garden Sprinkler Effect has been improved via the Booij and Holthuijsen (1987) technique (see also Tolman 2002c). Although not perfect (for example, the UQ scheme still has numerical error, and the GSE alleviation methods require tuning parameters that cannot be universal (see Tolman 2002c)), these might be considered "90% solutions" to the problems. This, combined with the fact that in this study we do not see much error associated with numerics even with the O(1) scheme of WAM4, leads us to believe that the "payoff" of further development would be small. Although again, if one looks at individual frequency components, numerical error is much more significant. Dissatisfaction with reliance on cancellation of errors (via spectral integration) may motivate further improvement of numerics.

Note that here we are primarily concerned with model skill. Certainly, it would be worthwhile to improve numerics such that computations are accelerated, e.g., by relaxing requirements on time step size.

7. SUMMARY

Findings of this study are summarized as follows.

1. Comparisons of the Navy WAM4 model to the Navy Swell Model hindcasts, and comparisons of hindcast results from the WvW3 model with first-order and higher-order numerics suggest that numerics and resolution are not dominant sources of error in predictions of low-frequency energy by the Navy's global wave models, even in cases of older swells, and even when O(1) numerics are used. However, the higher order numerics of WvW3 do result in more realistic images of swell field geographic distribution.

2. The physical formulations of the Navy's global wave models (i.e., WAM4 physics vs WvW3/TC physics) appear to play a more important role than numerics and resolution in predictions of low-frequency energy, but they still do not seem to be the dominant source of error. During the generation stage of the "life cycle" of wave energy, WAM4 is more energetic than WvW3 in shorter fetch/duration regimes, while the reverse is true in the longer fetch/duration regimes. In hindcasts, young swell events tend to peak slightly sooner in WAM4 and slightly higher in WvW3. However, despite the fairly consistent differences, our

hindcasts do not suggest that one formulation is consistently better at the growth stage. At the later, propagation stage of the life cycle of low-frequency wave energy, the TC physics used in the Navy's WvW3 model appear to be more skillful at dissipating swell correctly (WAM4 does not dissipate swell enough). However, since we ran only one hindcast case dealing with older swells in both WAM and WvW3 (July 2001), this particular conclusion is tentative.

3. The dominant source of error in predictions of low-frequency wave energy in the Navy's global models appears to be due to inaccuracies in the wind forcing. This is, in fact, consistent with the conclusion of Cardone et al. (1996). Specifically, the current operational implementation of the global atmospheric model (NOGAPS)–which produces the surface wind fields used to force the global wave models–has a tendency to underpredict the strength of high wind speed events. This is evident in comparisons to scatterometer data for two regions (North Pacific and southern Pacific Ocean) during winter months. This bias in the forcing leads to negative bias in predictions of low-frequency energy in both global wave models. This is dramatically demonstrated in the two "young swell" hindcasts shown here (January 2001 and January 2002, with comparisons to buoy data at the U.S. west coast). In the other hindcast (July 2001, with comparisons to buoy data at the mid-Pacific), comparisons are much more ambiguous, since none of the three forcing fields used produce consistently good results.

4. We have described a method of deriving wind forcing fields by blending scatterometer measurements with NOGAPS analyses. Despite the fact that the method is very simple (with several obvious manners in which it can be improved), we have shown that it can greatly alleviate the underprediction of low-frequency wave energy associated with the NOGAPS forcing bias. In hindcasts, this can improve predictions of both swell and wind sea, although it appears that one might get a similar benefit by employing NCEP winds in hindcasts. Used operationally at the Navy, this method of blended forcing (or an evolution thereof) might be used to improve forecasts of swell.

ACKNOWLEDGMENTS

Dr. James Kaihatu (NRL) is the Principal Investigator of the project that funded this investigation. Without his support, this work would not have been possible. Dr. Larry Hsu (NRL) was instrumental, as he provided Swell Model simulations and NAVO WAM model archives. His effort was funded by the Space and Naval Warfare Systems Command under the Coastal Wave and Surf Model Project. Paul Wittmann (FNMOC) provided sample input files for WvW3 (used to set up the NRL WvW3 hindcasts) and provided three WAM4 hindcast simulations. Richard Allard (NRL) provided the WAM4 code that was used to create the canonical WAM4 simulation presented herein. Pamela Posey (NRL) provided archives of FNMOC NOGAPS and COAMPS analyses. We thank NCEP, JPL, and Florida State University for providing their products free of charge by ftp. Collaboration with Drs. Paul Hwang and David Wang led to the SWAN work presented here. Conversations with Drs. Larry Hsu (NRL), David Wang (NRL), Hendrik Tolman (NCEP), Michael Schlax (Oregon State University), Mark Bourassa (FSU), Timothy Hogan (NRL), Keith Sashegyi (NRL), William O'Reilly (Scripps Institution of Oceanography), Peter Janssen (ECMWF), Cmdr. Raymond Robichaud, and others of NRL and the WISE (Waves In Shallow Environments) Group all provided useful information and discussions which contributed to this work. This work was funded by the Office of Naval Research via the Naval Research Laboratory Core Program, PE 62435N.

REFERENCES

Atlas, R., R.N. Hoffman, S.C. Bloom, J.C. Jusem, and J. Ardizzone, 1996: A Multi-year Global Surface Wind Velocity Data set Using SSM/I Wind Observations, *Bull. Amer. Meteorol. Soc.*, **77**, 869-882.

Atlas, R, R.N. Hoffman, S. M. Leidner, J. Sienkiewicz, T.-W. Yu, S.C. Bloom, E. Brin, J. Ardizzone, J. Terry, D. Bungato, and J.C. Jusem, 2001: The Effects of Marine Winds from Scatterometer Data on Weather Analysis and Forecasting, *Bull. Amer. Meteorol. Soc.*, **82**(9), 1965–1990.

Bender, L. C., 1996: Modification of the Physics and Numerics in a Third-generation Ocean Wave Model. *J. Atmos. Oceanic Technol.*, **13**, 726-750.

Bidlot, J-R, D.J. Holmes, P.A. Wittmann, R. Lalbeharry, and H.S. Chen, 2002: Intercomparison of the Performance of Operational Ocean Wave Forecasting Systems with Buoy Data, *Weather and Forecasting,* **17**(2), 287–310.

Booij, N., and L.H. Holthuijsen, 1987: Propagation of Ocean Waves in Discrete Spectral Wave Models. *J. Comput. Phys.*, **68**, 307-326.

Booij, N., R.C. Ris, and L.H. Holthuijsen, 1999: A Third-generation Wave Model for Coastal Regions, 1, Model Description and Validation. *J. Geophys. Res.*, **104**, 7649-7666.

Caplan, P., J. Derber, W. Gemmill, S.-Y. Hong, H.-L. Pan, and D. Parrish, 1997: Changes to the NCEP Operational Medium-Range Forecast Model Analysis-Forecast System. *Weather and Forecasting*, **12**, 581-594.

Daley, R. and E. Barker, 2001: *NRL Atmospheric Variational Data Assimilation System: Source Book 2001*. NRL/PU/7530—01-441, Naval Research Laboratory Washington, D.C.

Davis, R.W., and E.F. Moore, 1982: A Numerical Study of Vortex Shedding from Rectangles. *J. Fluid Mech.*, **116**, 475-506.

Dickinson, S., K. Kelly, M.J. Caruso, M.J. McPhaden, 2001: Comparisons between the TAO Buoy and NASA Scatterometer Wind Vectors. *J. Atm. Oceanic Tech.*, **18**, 799-806.

Freilich, M.H., and R.S. Dunbar, 1999: The Accuracy of the NSCAT 1 Vector Winds: Comparisons with National Data Buoy Center Buoys. *J. Geophys. Res.*, **104**(C5), 11231-11246.

Günther, H., S. Hasselmann and P.A.E.M. Janssen, 1992: The WAM Model Cycle 4 (Revised Version), *Deutsch. Klim. Rechenzentrum,* Techn. Rep. No. 4, Hamburg, Germany.

Hasselmann, K., 1974: On the Spectral Dissipation of Ocean Waves Due to Whitecapping. *Bound.-Layer Meteor.* **6**, 107-127.

Hasselmann, S., K. Hasselmann, J.H. Allender, and T.P. Barnett, 1985: Computations and Parameterizations of the Linear Energy Transfer in a Gravity Wave Spectrum, II, Parameterizations of the Nonlinear Transfer for Application in Wave Models. *J. Phys. Oceanogr.* **15**, 1378-1391.

Hodur, R.M., 1997: The Naval Research Laboratory's Coupled Ocean/Atmospheric Mesoscale Prediction System (COAMPS). *Mon. Wea. Rev.* **125**, 1414-1430.

Hodur, R.M., X. Hong, J.D. Doyle, J. Pullen, J. Cummings, P. Martin, and M.A. Rennick, 2002: The Coupled Ocean/Atmospheric Mesoscale Prediction System (COAMPS). *Oceanogr.*, **15**(1), 88-98.

Hogan, T.F., T.E. Rosmond, 1991: The Description of th U.S. Navy Operational Global Atmospheric Prediction System's Spectral Forecast Models. *Mon. Wea. Rev.* **119**, 1786-1815.

Holthuijsen, L.H., and N. Booij, 2000: Oceanic and Near-shore Whitecapping Effects in SWAN, *Sixth International Workshop on Wave Hindcasting and Forecasting, Monterey, CA,* Meteorological Service of Canada, 362-368.

Hsu, Y.L., W. E. Rogers, J.M. Kaihatu, R.A. Allard, 2000: Application of SWAN in the Mississippi Sound, *Sixth International Workshop on Wave Hindcasting and Forecasting, Monterey, CA,* Meteorological Service of Canada, 398-403.

Janssen, P.A.E.M., 1989: Wave-induced Stress and the Drag of Air Flow over Sea Waves. *J. Phys. Oceanogr.* **19**, 745-754.

Janssen, P.A.E.M., 1991: Quasi-linear Theory of Wind Wave Generation Applied to Wave Forecasting. *J. Phys. Oceanogr.* **21**, 1631-1642.

Janssen, P.A.E.M., P. Lionello, and L. Zambresky, 1989: On the Interaction of Wind and Waves. *Philos. Trans. Roy. Soc. London*, **A329**, 289-301.

Jensen, R.E., P. A. Wittmann, and J. D. Dykes, 2002: Global and Regional Wave Modeling Activities. *Oceanogr.* **15**(1), 57-66.

Kanamitsu, M., 1989: Description of the NMC Global Data Assimilation and Forecast System. *Wea. Forecasting*, **4**, 335-342.

Komen, G.J., L. Cavaleri, M. Donelan, K. Hasselmann, S. Hasselmann, and P.A.E.M. Janssen, 1994: *Dynamics and Modelling of Ocean Waves*. Cambridge Univ. Press, 532 pp.

Komen, G.J., S. Hasselmann, and K. Hasselmann, 1984: On the Existence of a Fully Developed Windsea Spectrum. *J. Phys. Oceanogr.* **14**, 1271-1285.

Leonard, B.P., 1979: A Stable and Accurate Convective Modeling Procedure Based on Quadratic Upstream Interpolation. *Comput. Meth. Appl. Mech. Eng.,* **19**, 59-98.

Leonard, B.P., 1991: The ULTIMATE Conservative Difference Scheme Applied to Unsteady Onedimensional Advection. *Comput. Methods Appl. Mech. Eng.* **88**, 17-74.

Moskowitz, L., 1964: Estimates of the Power Spectrums for Fully Developed Seas for Wind Speeds of 20 to 40 Knots. *J. Geophys. Res.* **69**(24), 5161-5179.

Pegion, P.J., M.A. Bourassa, D.M. Legler, and J.J. O'Brien, 2000: Objectively-derived Daily "Winds" from Satellite Scatterometer Data. *Mon. Wea. Rev.* **128**, 3150-3168.

Pierson, W.J., and L. Moskowitz, 1964: A Proposed Spectral form for Fully Developed Wind Seas Based on the Similarity Theory of S.A. Kitaigorodskii. *J. Geophys. Res.* **69**(24), 5181-5190.

Phillips, O.M., 1985: Spectral and Statistical Properties of the Equilibrium Range in Wind-generated Gravity Waves. *J. Fluid Mech.,* **156**, 505-531.

PODAAC (Physical Oceanography Distributed Active Archive Center), 2001a: *QuikSCAT Science Data Product User's Manual*. Jet Propulsion Laboratory Technical Document. 86 pp.

PODAAC (Physical Oceanography Distributed Active Archive Center), 2001b: *SeaWinds on QuikSCAT Level 3 Daily, Gridded Ocean Wind Vectors (JPL SeaWinds Project)*. Jet Propulsion Laboratory Technical Document. 39 pp.

Portabella, M., A. Stoffelen, 2001: Rain Detection and Quality Control of SeaWinds. *J. Atmos. Oceanic Tech.* **18**, 1171-1183.

Rogers, W.E, and W.C. O'Reilly, 2001: Pacific Basin Wind-wave Models: The Generation and Decay of Low Frequency Energy. *Proceedings of the Fourth International Symposium; Ocean Wave Measurement and Analysis (WAVES 2001),* San Francisco, CA, ASCE, 934-943.

Rogers, W.E., P. A. Hwang, and D. W. Wang, 2002a: Investigation of Wave Growth and Decay in the SWAN Model: Three Regional-Scale Applications, accepted for publication, *J. Phys. Oceanogr.*

Rogers, W.E., J.M. Kaihatu, H.A.H. Petit, N. Booij, L.H Holthuijsen, 2002b: Diffusion Reduction in an Arbitrary Scale Third Generation Wind Wave Model. *Ocean Eng.* **29**, 1357-1390.

Rosmond, T.E., J. Teixeira, M. Peng, T.F. Hogan, R. Pauley, 2002: Navy Operational Global Atmospheric Prediction System (NOGAPS): Forcing for Ocean Models. *Oceanogr.* **15**(1), 99-108.

Schlax, M.G., D.B. Chelton, M.H. Freilich, 2001: Sampling Errors in Wind Fields Constructed from Single and Tandem Scatterometer Datasets. *J. Atmos. Ocean. Tech.* **18**, 1014-1036.

Tolman, H.L., 1991: A Third Generation Model for Wind Waves on Slowly Varying, Unsteady and Inhomogeneous Depths and Currents. *J. Phys. Oceanogr.* **21**, 782-797.

Tolman, H.L., 1995: On the Selection of Propagation Schemes for a Spectral Wind-wave Model. NWS/NCEP Office Note 411, 30 pp. + figures.*

Tolman, H.L, 1998: Validation of NCEP's Ocean Winds for Use in Wind Wave Models. *The Global Atmospheric and Ocean System,* **6**, 243-268.

Tolman, H.L, 1999: *User Manual and System Documentation of WAVEWATCH-III Version 1.18*. NCEP Technical Note. 110 pp.*

Tolman, H.L., 2001: Improving Propagation in Oocean Wave Mmodels. *Proceedings of the Fourth International Symposium; Ocean Wave Measurement and Analysis (WAVES 2001),* San Francisco, CA, ASCE, 507-516.

Tolman, H.L., 2002: *Validation of WAVEWATCH III Version 1.15 for a Global Domain*. NCEP Technical Note, 33 pp.*

Tolman, H.L. and D. Chalikov, 1996: Source Terms in a Third-generation Wind Wave Model. *J. Phys. Oceanogr*. **26**, 2497-2518.

Tolman, H.L., B. Balasubramaniyan, L.D. Burroughs, D.V. Chalikov, Y.Y. Chao, H.S. Chen, and V.M. Gerald, 2002: Development and Implementation of Wind-generated Ocean Surface Wave Models at NCEP. *Weather and Forecasting (NCEP Notes)*, **17**, 311-333.

Van Vledder, G. Ph. 1999: *Source Term Investigation: SWAN*, Rev. 2, Report number A162R1r2, Alkyon, 83 pp. + figures.

Van Vledder, G. Ph., T. H. C. Herbers, R. E. Jensen, D. T. Resio and B. Tracy, 2000: Modeling of Non-linear Quadruplet Wave-wave Interactions in Operational Models. *Proceedings, 27th International Conference on Coastal Engineering*, Sydney, Australia, ASCE, 797-811.

WAMDI Group, 1988: The WAM model—A Third Generation Ocean Wave Prediction Model. *J. Phys. Oceanogr.* **18**, 1775-1810.

Wingeart, K.M., T.H.C. Herbers, W.C. O'Reilly, P.A. Wittmann, R.E. Jensen, H.L. Tolman, 2001: Validation of Ooperational Global Wave Prediction Models with Spectral Buoy Data. *Proceedings of the Fourth International Symposium; Ocean Wave Measurement and Analysis (WAVES 2001),* San Francisco, CA, ASCE, 590-599.

Wittmann, P.A., 2001: Implementation of WAVEWATCH-III at Fleet Numerical Meteorological and Oceanography Center. *Conference proceedings: MTS/IEEE Conference and Exposition: An Ocean Odyssey: November 5-8, 2001, Honolulu, Hawaii (sponsored by Marine Technology Society and IEEE)*, 1474-1479.

Wittmann, P.A., and W.C. O'Reilly, 1998: WAM Validation of Pacific Swell. *5th International Workshop on Wave Hindcasting and Forecasting*. Melbourne FL, Atmospheric Environmental Service, Downsview Ontario, Canada, 83-87.

Wittmann, P. A. and R. M. Clancy, 1993: Implementation and Validation of a Global Third-generation Wave Model at Fleet Numerical Oceanography Center. In *Proc. 2nd International Symp. Ocean Wave Measurement and Analysis*, New Orleans, Louisiana, 406-419.

Wittmann, P.A, R.M. Clancy, and T. Mettlach, 1995: Operational Wave Forecasting at Fleet Numerical Meteorology and Oceanography Center. In *Proc. 4th International Workshop on Wave Hindcasting and Forecasting*, Banff, Alberta, Canada, 335-342.

* The NCEP Technical Notes are not formally published, but electronic versions are available for download from NCEP.

Appendix A
PHYSICAL FORMULATIONS IN THE SWAN MODEL

The investigations described in this appendix are taken from the work of Rogers et al. (2002a) (henceforth RHW). Some of the work described here appears in that article. The dissipation term of the SWAN model is that of WAM, Cycles 1-3 (WAMDI Group 1988), which can be described by

$$S_{ds}(\sigma,\theta) = C_{ds}\left[\frac{s}{s_{PM}}\right]^{m} \sigma_m \left(\frac{k}{k_m}\right)^{n} E(\sigma,\theta) \quad , \tag{A1}$$

where C_{ds} is an empirical coefficient of proportionality, s is the overall wave steepness, $s = k_m \sqrt{E_{tot}}$, the subscript m denotes mean, k is wavenumber, and subscript PM denotes the fully-developed sea state (as defined by Pierson and Moskowitz (1964)), for which s is assumed to be a constant. The SWAN model and WAM Cycles 1-3 use n = 1. based on Komen et al. (1984) and Hasselmann (1974), who theorizes that since the wave scales are large compared with the whitecap dimension, the dissipation coefficient should be proportional to the square of the frequency (i.e., n = 1).

RHW note a consistent bias in energy of the SWAN model: negative at lower frequencies and positive at higher frequencies. This bias is, to some extent, balanced out when one looks at total energy (i.e., wave height), but it has a marked effect on predictions of mean wave period (or wave number). RHW also note that because of the form of Eq. (A1), this bias might be easily corrected by increasing n (which has the effect of increasing dissipation on higher wavenumbers and decreasing dissipation of lower wavenumbers). RHW apply the SWAN model with n = 2 (and the other free parameters unchanged) to three hindcasts of moderate to strong wind events (e.g., U_{10} = 10-20 m/s) at regional/subregional scale (O(100 km × 100 km) domain size), and note greatly improved results (see Section A1).

During a review of the literature, RHW discovered that Janssen et al. (1989), using the WAM model with the whitecap model of Eq. (6), report too much energy in the higher frequencies using n = 1 and more satisfactory results using n = 2. Janssen et al. (1989) argue that the assumption that wave scales are large compared to the whitecap scale is not necessarily valid, especially in the higher frequency range. Based on this, one might envision a formulation where n is dependent on frequency or wave age (equal to unity at lower frequencies, diverging at the higher frequencies). However, Janssen et al. (1989), like RHW, take the simpler approach of applying a larger value of n uniformly.

Developing the arguments of Janssen et al. (1989), RHW propose a more physically justified (and more novel) modification:

$$\begin{cases} n = 1 & k \le k_m \\ n = n_2 & k > k_m \end{cases} , \tag{A2}$$

although they do not repeat their hindcasts with this modification. There is no guidance for n_2. We extend the work of RHW by repeating their hindcasts using this modification, with $n_2 = 2$.

Other possible forms might be taken. For example, n_2 might be a tunable (empirical) function of several parameters, such as wave age; the free parameters used in the Tolman and Chalikov dissipation term might be a good starting point. Another approach would be to use the "equilibrium range" dissipation term form of Phillips (1985) where $k > k_m$ (rather than Eq. (A1)).

Although at first glance it might appear that the underprediction of low-frequency energy would not be corrected by modification (Eq. (A2)) (since the low-frequency n is unchanged), our tests reveal that it *is* corrected, to a large extent. The explanation is simple: the underprediction of low-frequency energy can be attributed to bulk parameters (e.g., mean steepness) that are influenced by the overprediction of high-frequency energy. By dissipating the high-frequency energy more, we indirectly reduce dissipation on low frequencies.

Note that although this type of modification is more physically appropriate than applying $n = 2$ everywhere in the spectrum, it unfortunately still leaves more fundamental problems with the KHH form, namely excessive dependence on spectrum-integrated terms. Thus, this potential evolutionary development of the KHH form cannot be a final solution.

SWAN Hindcasts

The three hindcast simulations were of

- a two-part Lake Michigan storm event during Nov. 9-13, 1995,
- a very "clean" fetch-limited growth case in the Mississippi Bight during October 1999, and
- a moderate strength wind event of SandyDuck '97, 23-25 September 1997. RHW use interpolated buoy wind measurements for model forcing (and in the case of the SandyDuck simulation, boundary (swell) forcing is also included, again based on buoy measurements). The wind conditions of the Lake Michigan and Mississippi Bight simulations are believed to be very well described, but less so in the case of the SandyDuck simulation (due to complexity of winds in that case). Table A1 describes the three hindcasts at a glance. RHW provide additional detail on the simulations.

Other "options:"

- higher order numerics (no effect)
- smaller time step (no effect)
- For SandyDuck case, a nested (more high-resolution) case was also run, but this increased resolution did not affect presented results.

Variations of whitecapping formulation

- SWAN default ($n = 1.0$, $C_{ds} = 2.36 \times 10^{-5}$)
- Increased n, C_{ds} not altered ($n = 2.0$, $C_{ds} = 2.36 \times 10^{-5}$)
- Hybrid model, using (A2) with $n_2 = 2$.

Table A1 – Options and other model controls used in the three regional-scale SWAN hindcasts.

Case	Lake Michigan	Mississippi Bight	SandyDuck
Nonstationary?	Yes	Yes	Yes
Δt	10 min.	10 min.	10 min.
Nx	127	81	151 (outer nest)
Δx	2000 m	3630 m	2000 m (outer nest)
Ny	249	41	261 (outer nest)
Δy	2000 m	4720 m	2000 m (outer nest)
$n\theta$	36	36	36
$\Delta\theta$	10°	10°	10°
$n\sigma$	34	36	34
σ_l (lowest modeled frequency)	0.07 Hz	0.08 Hz	0.05 Hz
σ_h (highest modeled frequency)	1.00 Hz	1.00 Hz	1.00 Hz
Wind forcing?	Yes (from 2 buoys)	Yes (from 1 buoy)	Yes (from 3 buoys)
Boundary forcing?	No (entire lake included)	No (insignificant amount of swell during this period)	Yes (swell only; stationary)
Initial condition	Rest	Rest	Produced using stationary computation with no winds (boundary forcing only) to fill domain with "background swell".
Bottom friction	SWAN default (JONSWAP)		
Triads?	Yes (default settings for SWAN triads formulation), but did not affect results presented.		
Numerics	Default for v40.01 (e.g., first order geographic propagation)		
S_{in} term	SWAN default (WAM3)		

The results are shown in Fig. A1. The figures are actually complimentary to those given by RHW, since RHW present only detailed time series of frequency spectra, not bulk parameters. In general, mean period prediction is dramatically improved by the modifications, while prediction of peak period and total energy is more modestly improved. As expected, the $n = 2$ model results in the greatest differences (vs the original model), but the hybrid model is generally fairly close to the $n = 2$ model.

A2. Canonical Cases

Canonical applications of the SWAN model–analogous to those presented in Section 3 for WAM and WvW3–are presented here (see Fig. A2). Note that the SWAN model with WAM3 physics, although similar, is not identical to the WvW3 model with WAM3 physics. This is expected because of the differences in model implementation (e.g., numerical implementation of source/sink terms, handling of high-frequency tail, etc.). The similarity between the modified ($n = 2$) SWAN model and the WAM4 result is remarkable.

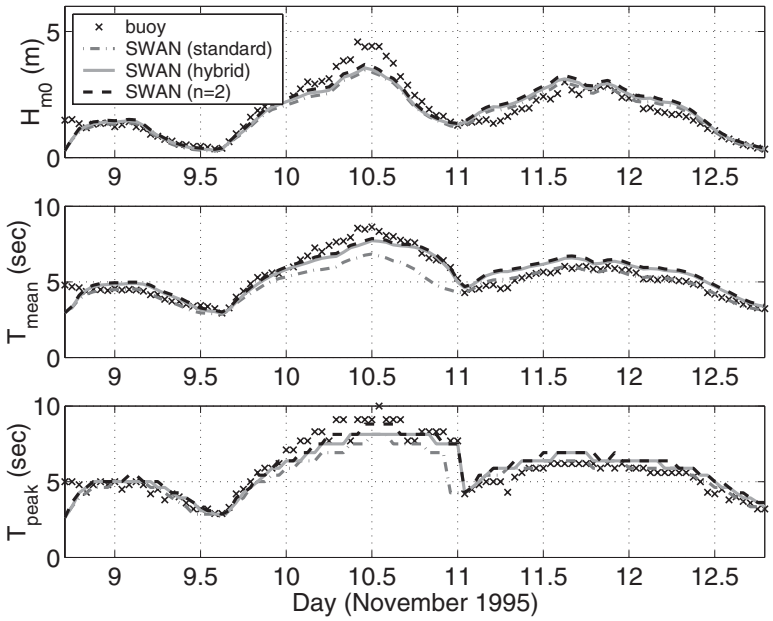

(a) Lake Michigan simulation, location of NDBC buoy 45002. Frequency interval 0.07 to 0.4Hz used in wave height, mean period calculations

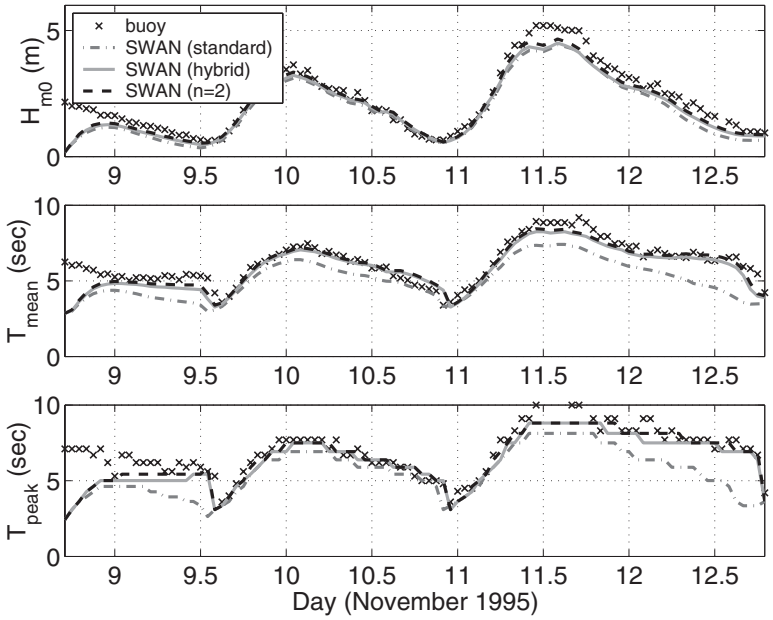

(b) Lake Michigan simulation, location of NDBC buoy 45007

Fig. A1(a-d) — Comparison of SWAN model hindcasts vs buoy data using three different dissipation formulations [n = 1, n = 2, and hybrid n]. Zero moment wave height, mean period, and peak period are shown.

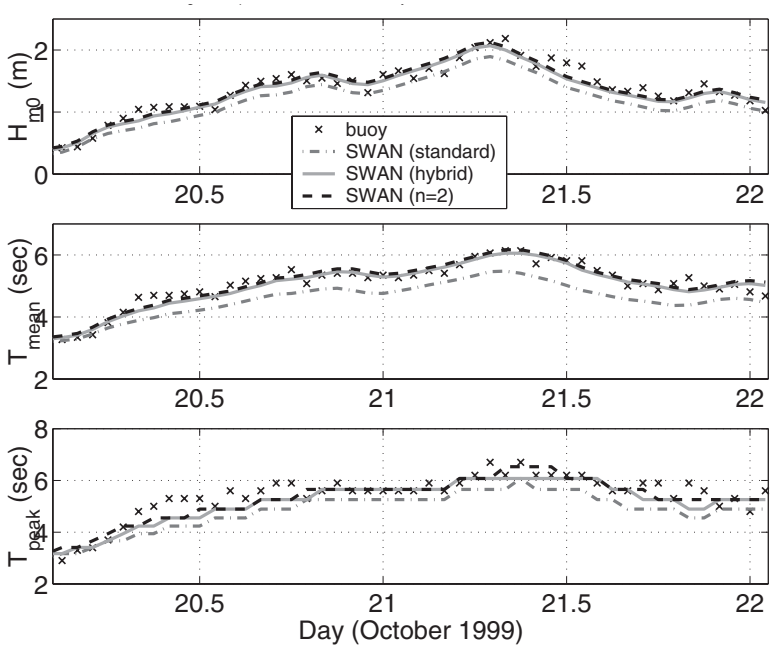

(c) Mississippi Bight simulation, location of NDBC buoy 42040. Frequency interval 0.08 to 0.35Hz used in wave height, mean period calculations.

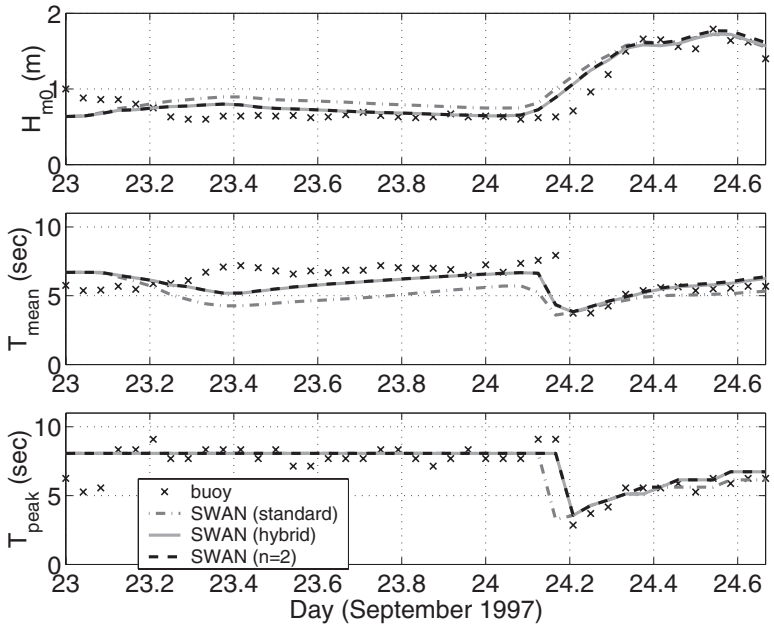

(d) SandyDuck '97 simulation, location of NDBC buoy 44014. Frequency interval 0.05 to 0.4 Hz used in mean period calculations.

Fig. A1(a-d) (Continued) — Comparison of SWAN model hindcasts vs buoy data using three different dissipation formulations [$n = 1$, $n = 2$, and hybrid n]. Zero moment wave height, mean period, and peak period are shown.

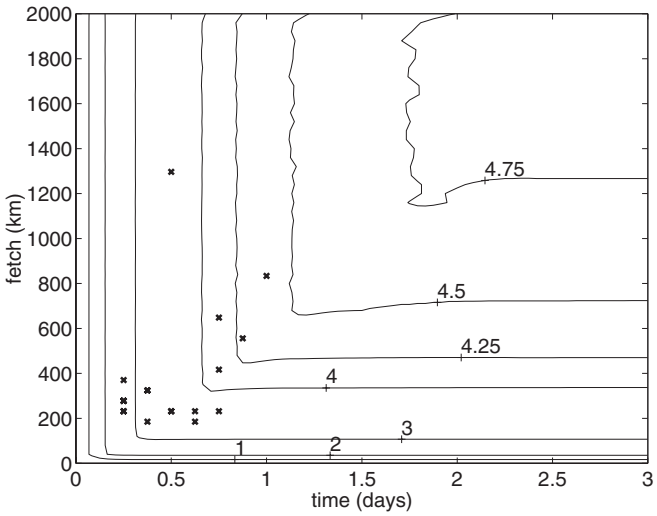

(a) Standard SWAN dissipation formulation (n = 1)

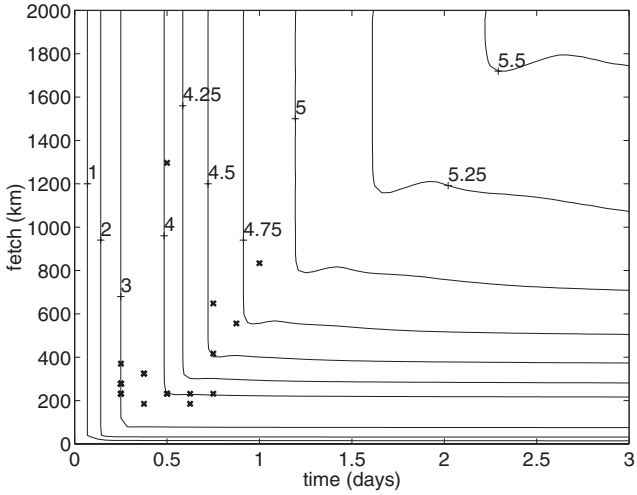

(b) n = 2

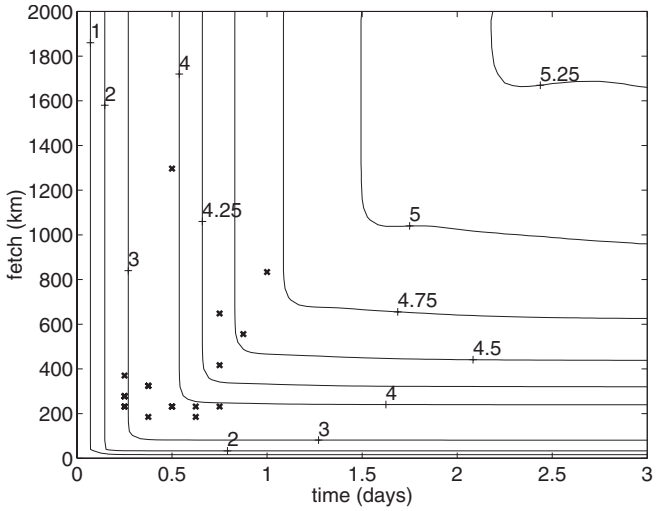

(c) hybrid n

Fig. A2(a-c) — Same as Fig. 3, except SWAN results shown

A3. Discussion

Some relevant observations and discussions made by RHW are included here.

Tuning Techniques

The "classical method" of tuning a wind-wave model is to tune to empirical fetch-limited growth curves, or to some fetch-unlimited, duration-unlimited condition, such as the Pierson-Moskowitz spectrum. (The latter approach was taken by Komen et al. (1984) when designing the WAM Cycles 1-3 S_{in} and S_{ds}, for example). In both cases, duration-limited conditions are ignored (i.e., the rate at which models reach their respective asymptotes is not considered). Furthermore, mean period is ignored. A possible alternative to the classical method is to tune models to several hindcasts in which the temporal behavior of wave spectra are well described. This is a logical evolutionary step in wave model development. RHW did not pursue such tuning, but it would be possible to do so by using a large set of hindcasts such as the Lake Michigan and Mississippi Bight cases. Unfortunately, because of inaccuracies associated with the DIA, it may be impossible to create a "general tuning" for these models, applicable at any scale (see also discussion in Tolman 2002a). And in fact, in the context of SWAN, aspects of the other source terms may create problems when attempting to create a tuning that is general for any scale; for example, the dissipation term's excessive reliance on spectrum-integrated parameters. The source terms probably should be developed at the scales at which they will be applied (e.g., tuning to short-fetch empirical growth curves probably will not produce a skillful global model).

Aphysical Influence of Integrated Parameters on S_{ds}

The dissipation terms of SWAN and WAM rely on spectrum-integrated parameters. Thus the presence of wind sea can have an illogical and physically unjustified impact on swell, and vice versa. The effect of swell on wind sea in the SWAN model is being addressed (see Van Vledder (1999) and Holthuijsen and Booij (2000), for example). The reverse effect has not been addressed. RHW demonstrate that it can have a dramatic effect in the SWAN model. In the WAM4 model, on the other hand, the effect appears to be much more modest (Peter Janssen, personal communication). HW propose a correction to the SWAN model (by disallowing the dissipation of swell via the whitecapping term). The criterion is effective at identifying low-steepness swells ($H_{swell} < 1$ m, approximately) and preventing the aphysical dissipation, but the definition of "swell" in this modification requires further development. In its present form, improvements to cases with steeper swells show only modest improvements (a direct result of safeguards intended to minimize occurrence of excessive growth or oddlyshaped spectra).

Appendix B

HINDCAST COMPARISONS USING ALTERNATE FREQUENCY RANGES

In Section 5, we defined low-frequency wave height as the wave height based on variance (energy) up 0.08 Hz, and presented tables comparing various hindcasts using error measures based on this wave height definition. Here, we present analogous tables, but with two alternate definitions of low: 0.06 Hz and 0.10 Hz. Note that since the 0.10 Hz wave height is closer to the total wave height than is the 0.08Hz wave height, we can expect that resulting skill measures would be more similar to that derived from altimeter comparisons. The 0.06 Hz wave heights are more swell-dominated than are the 0.08Hz wave heights.

In all tables, models are ranked according to skill for that particular comparison.

B1. Numerical Scheme and Source/Sink Term: Sensitivity

Table B1(a) — Error measures based on energy up to 0.06 Hz for January 2001 hindcast at location of NDBC buoy 46059 (west of San Francisco). Hindcasts with NOGAPS forcing are shown. (WAM4 result provided by Larry Hsu, NRL)

January 2001. NOGAPS forcing. Buoy 46059. H_{m0} based on energy up to 0.06 Hz				
Model Platform	Numerics	Physics	Bias (m)	RMSE (m)
WAM4	O(1)	WAM4	–0.88	1.23
WvW3	UQ	TC	–1.20	1.56
WvW3	O(1)	TC	–1.25	1.62
WvW3	O(1)	KHH	–1.36	1.74
WvW3	UQ	KHH	–1.41	1.77

Table B1(b) — Same as Table B1(a), but for spectral energy up to 0.10 Hz

January 2001. NOGAPS forcing. Buoy 46059. H_{m0} based on energy up to 0.10 Hz				
Model platform	Numerics	Physics	Bias (m)	RMSE (m)
WAM4	O(1)	WAM4	–0.96	1.35
WvW3	UQ	TC	–1.01	1.53
WvW3	O(1)	TC	–1.04	1.59
WvW3	O(1)	KHH	–2.09	2.42
WvW3	UQ	KHH	–2.15	2.45

Table B2(a) — Error measures based on energy up to 0.06 Hz for January 2001 hindcast at location of NDBC buoy 46059 (west of San Francisco). Hindcasts with NCEP forcing are shown.

January 2001. NCEP forcing. Buoy 46059. WvW3 model. H_{m0} based on energy up to 0.06 Hz		
Numerics	Physics	Bias (m)
O(1)	TC	–0.70
UQ	TC	–0.71
O(1)	KHH	–1.02
UQ	KHH	–1.03
Numerics	Physics	RMSE (m)
UQ	TC	1.01
O(1)	TC	1.05
UQ	KHH	1.28
O(1)	KHH	1.30

Table B2(b) — Same as Table B2(a), but for spectral energy up to 0.10 Hz

January 2001. NCEP Forcing. Buoy 46059. WvW3 model. H_{m0} based on energy up to 0.10 Hz		
Numerics	Physics	Bias (m)
O(1)	TC	–0.15
UQ	TC	–0.18
O(1)	KHH	–1.32
UQ	KHH	–1.36
Numerics	Physics	RMSE (m)
UQ	TC	0.67
O(1)	TC	0.70
O(1)	KHH	1.54
UQ	KHH	1.56

Table B3(a) — Error measures based on energy up to 0.06 Hz for July 2001 hindcast at location of NDBC buoy 51028 (Christmas Island). Hindcasts with NOGAPS forcing are shown. (WAM4 result provided by Larry Hsu, NRL)

July 2001. NOGAPS forcing. Buoy 51028. H_{m0} based on energy up to 0.06 Hz.			
Model Platform	Numerics	Physics	Bias (m)
WvW3	UQ	TC	–0.22
WAM4	O(1)	WAM4	–0.23
WvW3	O(1)	TC	–0.24
Model Platform	Numerics	Physics	RMSE (m)
WvW3	UQ	TC	0.26
WvW3	O(1)	TC	0.28
WAM4	O(1)	WAM4	0.30

Table B3(b) — Same as Table B3(a), but for spectral energy up to 0.10 Hz

July 2001. NOGAPS forcing. Buoy 51028. H_{m0} based on energy up to 0.10 Hz			
Model Platform	Numerics	Physics	Bias (m)
WAM4	O(1)	WAM4	0.10
WvW3	UQ	TC	–0.11
WvW3	O(1)	TC	–0.16
Model Platform	Numerics	Physics	RMSE (m)
WvW3	UQ	TC	0.23
WvW3	O(1)	TC	0.26
WAM4	O(1)	WAM4	0.26

Table B4(a) — Error measures based on energy up to 0.06 Hz for July 2001 hindcast at location of NDBC buoy 51028 (Christmas Island). Hindcasts with NCEP forcing are shown. (WAM4 result provided by Paul Wittmann, FNMOC)

July 2001. NCEP forcing. Buoy 51028. H_{m0} based on energy up to 0.06 Hz.			
Model Platform	Numerics	Physics	Bias (m)
WvW3	UQ	TC	–0.01
WAM4	O(1)	WAM4	0.04
WvW3	O(1)	TC	–0.05
Model Platform	Numerics	Physics	RMSE (m)
WvW3	O(1)	TC	0.11
WvW3	UQ	TC	0.12
WAM4	O(1)	WAM4	0.13

Table B4(b) — Same as Table B4(a), but for spectral energy up to 0.10 Hz

July 2001. NCEP model. Buoy 51028. H_{m0} based on energy up to 0.10 Hz.				
Model Platform	Numerics	Physics	Bias (m)	RMSE (m)
WvW3	O(1)	TC	0.20	0.26
WvW3	UQ	TC	0.26	0.31
WAM4	O(1)	O(1)	0.49	0.52

Table B5(a) — Error measures based on energy up to 0.06 Hz for July 2001 hindcast at location of NDBC buoy 46059 (west of San Francisco). Hindcasts with NOGAPS forcing are shown. (WAM4 result provided by Larry Hsu, NRL)

July 2001. NOGAPS forcing. Buoy 46059. H_{m0} based on energy up to 0.06 Hz				
Model Platform	Numerics	Physics	Bias (m)	RMSE (m)
WAM4	O(1)	WAM4	–0.08	0.14
WvW3	UQ	TC	–0.14	0.20
WvW3	O(1)	TC	–0.15	0.21

Table B5(b) — Same as Table B5(a), but for spectral energy up to 0.10 Hz

July 2001. NOGAPS forcing. Buoy 46059. H_{m0} based on energy up to 0.10 Hz			
Model Platform	Numerics	Physics	Bias (m)
WvW3	UQ	TC	–0.18
WvW3	O(1)	TC	–0.19
WAM4	O(1)	WAM4	0.43
Model Platform	Numerics	Physics	RMSE (m)
WvW3	O(1)	TC	0.37
WvW3	UQ	TC	0.38
WAM4	O(1)	WAM4	0.49

Table B6(a) — Error measures based on energy up to 0.06 Hz for July 2001 hindcast at location of NDBC buoy 46059 (west of San Francisco). Hindcasts with NCEP forcing are shown. (WAM4 result provided by Paul Wittmann, FNMOC)

July 2001. NCEP forcing. Buoy 46059. H_{m0} based on energy up to 0.06 Hz				
Model platform	Numerics	Physics	Bias (m)	RMSE (m)
WvW3	O(1)	TC	0.01	0.11
WvW3	UQ	TC	0.02	0.13
WAM4	O(1)	WAM4	0.19	0.23

Table B6(b) — Same as Table B6(a), but for spectral energy up to 0.10 Hz

July 2001. NCEP forcing. Buoy 46059. H_{m0} based on energy up to 0.10 Hz				
Model platform	Numerics	Physics	Bias (m)	RMSE (m)
WvW3	O(1)	TC	0.08	0.26
WvW3	UQ	TC	0.09	0.27
WAM4	O(1)	WAM4	0.65	0.72

B2. Impact of Forcing: Degree of Data Usage in Blended NOGAPS/QuikSCAT Fields

Table B7(a) — Error measures based on energy up to 0.06 Hz for January 2001 hindcast at location of NDBC buoy 46059 (west of San Francisco). WvW3 hindcasts (default physics (TC) and numerics (UQ)) with varying degrees of data usage in forcing are shown (NOGAPS background).

January 2001. WvW3 model. Buoy 46059. H_{m0} based on energy up to 0.06 Hz		
Forcing	Bias (m)	RMSE (m)
L3 (W∞)	–0.39	0.69
NOGAPS+QuikSCAT (L2B, W6)	–0.50	0.72
NOGAPS+QuikSCAT (L2B, W3)	–0.91	1.18
NOGAPS	–1.20	1.56

Table B7(b) — Same as Table B7(a), but for spectral energy up to 0.10 Hz

January 2001. WvW3 model. Buoy 46059. H_{m0} based on energy up to 0.10 Hz		
Forcing	Bias (m)	RMSE (m)
NOGAPS+QuikSCAT (L2B, W6)	0.22	0.74
NOGAPS+QuikSCAT (L2B, W3)	–0.41	0.81
L3 (W∞)	0.44	0.90
NOGAPS	–1.01	1.53

Table B8(a) — Error measures based on energy up to 0.06 Hz for July 2001 hindcast at location of NDBC buoy 51028 (Christmas Island). WvW3 hindcasts (default physics (TC) and numerics (UQ)) with varying degrees of data usage in forcing are shown (NOGAPS background).

July 2001. WvW3 model. Buoy 51028. H_{m0} based on energy up to 0.06 Hz		
Forcing	Bias (m)	RMSE (m)
NOGAPS+QuikSCAT (L2B, W3)	–0.07	0.13
NOGAPS+QuikSCAT (L2B, W6)	0.10	0.21
L3 (W∞)	0.18	0.26
NOGAPS	–0.22	0.26

Table B8(b) — Same as Table B8(a), but for spectral energy up to 0.10 Hz

July 2001. WvW3 model. Buoy 51028. H_{m0} based on energy up to 0.10 Hz		
Forcing	Bias (m)	RMSE (m)
NOGAPS	–0.11	0.23
NOGAPS+QuikSCAT (L2B, W3)	0.18	0.25
NOGAPS+QuikSCAT (L2B, W6)	0.45	0.50
L3 (W∞)	0.71	0.73

Table B9(a) — Error measures based on energy up to 0.06 Hz for July 2001 hindcast at location of NDBC buoy 46059 (west of San Francisco). WvW3 hindcasts (default physics (TC) and numerics (UQ)) with varying degrees of data usage in forcing are shown (NOGAPS background).

July 2001. WvW3 model. Buoy 46059. H_{m0} based on energy up to 0.06 Hz		
Forcing	Bias (m)	RMSE (m)
NOGAPS+QuikSCAT (L2B, W3)	–0.02	0.12
NOGAPS+QuikSCAT (L2B, W6)	0.12	0.20
NOGAPS	–0.14	0.20
L3 (W∞)	0.18	0.25

Table B9(b) — Same as Table B9(a), but for spectral energy up to 0.10 Hz

July 2001. WvW3 model. Buoy 46059. H_{m0} based on energy up to 0.10 Hz		
Forcing	Bias (m)	RMSE (m)
NOGAPS+QuikSCAT (L2B, W3)	0.07	0.28
NOGAPS	–0.18	0.38
NOGAPS+QuikSCAT (L2B, W6)	0.33	0.40
L3 (W∞)	0.46	0.51

B3. Impact of Forcing: Atmospherics Model Analyses vs Blended NOGAPS/QuikSCAT Fields

Table B10(a) — Error measures based on energy up to 0.06 Hz for January 2001 hindcast at location of NDBC buoy 46059 (west of San Francisco). WvW3 hindcasts (default physics (TC) and numerics (UQ)) with different forcing fields are shown.

January 2001. WvW3 model (default physics/numerics). Buoy 46059. H_{m0} based on energy up to 0.06 Hz		
Forcing	Bias (m)	RMSE (m)
NOGAPS+QuikSCAT (L2B, W6)	–0.50	0.72
NCEP	–0.71	1.01
NOGAPS/COAMPS	–1.07	1.34
NOGAPS	–1.20	1.56

Table B10(b) — Same as Table B10(a), but for spectral energy up to 0.10 Hz

January 2001. WvW3 model (default physics/numerics). Buoy 46059. H_{m0} based on energy up to 0.10 Hz		
Forcing	Bias (m)	RMSE (m)
NCEP	–0.18	0.67
NOGAPS+QuikSCAT (L2B, W6)	0.22	0.74
NOGAPS/COAMPS	–0.58	1.04
NOGAPS	–1.01	1.53

Table B11(a) — Error measures based on energy up to 0.06 Hz for July 2001 hindcast at location of NDBC buoy 51028 (Christmas Island). WvW3 hindcasts (default physics (TC) and numerics (UQ)) with different forcing fields are shown.

July 2001. WvW3 model (default physics/numerics). Buoy 51028. H_{m0} based on energy up to 0.06 Hz		
Forcing	Bias (m)	RMSE (m)
NCEP	–0.01	0.12
NOGAPS+QuikSCAT (L2B, W6)	0.10	0.21
NOGAPS	–0.22	0.26

Table B11(b) — Same as Table B11(a), but for spectral energy up to 0.10 Hz

July 2001. WvW3 model (default physics/numerics). Buoy 51028. H_{m0} based on energy up to 0.10 Hz		
Forcing	Bias (m)	RMSE (m)
NOGAPS	–0.11	0.23
NCEP	0.26	0.31
NOGAPS+QuikSCAT (L2B, W6)	0.45	0.50

Table B12(a) — Error measures based on energy up to 0.06 Hz for July 2001 hindcast at location of NDBC buoy 51028 (Christmas Island). WAM4 hindcasts with different forcing fields are shown. (WAM4 results were provided by Larry Hsu, NRL and Paul Wittmann, FNMOC.)

July 2001. WAM4 model. Buoy 51028. H_{m0} based on energy up to 0.06 Hz		
Forcing	Bias (m)	RMSE (m)
NCEP	0.04	0.13
NOGAPS	–0.23	0.30

Table B12(b) — Same as Table B12(a), but for spectral energy up to 0.10 Hz

July 2001. WAM4 model. Buoy 51028. H_{m0} based on energy up to 0.10 Hz		
Forcing	Bias (m)	RMSE (m)
NOGAPS	0.10	0.26
NCEP	0.49	0.52

Table B13(a) — Error measures based on energy up to 0.06 Hz for July 2001 hindcast at location of NDBC buoy 46059 (west of San Francisco). WvW3 hindcasts (default physics (TC) and numerics (UQ)) with different forcing fields are shown.

July 2001. WvW3 model (default physics/numerics). Buoy 46059. H_{m0} based on energy up to 0.06 Hz		
Forcing	Bias (m)	RMSE (m)
NCEP	0.02	0.13
NOGAPS+QuikSCAT (L2B, W6)	0.12	0.20
NOGAPS	–0.14	0.20

Table B13(b) — Same as Table B13(a), but for spectral energy up to 0.10 Hz

July 2001. WvW3 model (default physics/numerics). Buoy 46059. H_{m0} based on energy up to 0.10 Hz		
Forcing	Bias (m)	RMSE (m)
NCEP	0.09	0.27
NOGAPS	–0.18	0.38
NOGAPS+QuikSCAT (L2B, W6)	0.33	0.40

Table B14(a) — Error measures based on energy up to 0.06 Hz for July 2001 hindcast at location of NDBC buoy 46059 (west of San Francisco). WAM4 hindcasts with different forcing fields are shown. (WAM4 results were provided by Larry Hsu (NRL) and Paul Wittmann (FNMOC).)

July 2001. WAM4 model. Buoy 46059. H_{m0} based on energy up to 0.06 Hz		
Forcing	Bias (m)	RMSE (m)
NOGAPS	–0.08	0.14
NCEP	0.19	0.23

Table B14(b) — Same as Table B14(a), but for spectral energy up to 0.10 Hz

July 2001. WAM4 model. Buoy 46059. H_{m0} based on energy up to 0.10 Hz		
Forcing	Bias (m)	RMSE (m)
NOGAPS	0.43	0.49
NCEP	0.65	0.72

B4. Repeatability Check: January 2002

Table B15(a) — Error measures based on energy up to 0.06 Hz for January 2002 hindcast at location of NDBC buoy 46006 (west of Northern California). (WAM4 results were provided by Larry Hsu (NRL) and Paul Wittmann (FNMOC))

January 2002. Buoy 46006. H_{m0} based on energy up to 0.06 Hz.			
Model Platform (default physics/numerics)	Forcing	Bias (m)	RMSE (m)
WAM4	NCEP	–0.18	0.50
WvW3	NOGAPS+QuikSCAT (L2B, W6)	–0.20	0.51
WvW3	NCEP	–0.29	0.58
WAM4	NOGAPS	–0.62	0.94
WvW3	NOGAPS	–0.67	0.98

Table B15(b) — Same as Table B15(a), but for spectral energy up to 0.10 Hz

Model Platform (default physics/numerics)	Forcing	Bias (m)
WAM4	NCEP	–0.11
WvW3	NCEP	0.14
WvW3	NOGAPS+QuikSCAT (L2B, W6)	0.23
WvW3	NOGAPS	–0.48
WAM4	NOGAPS	–0.65
Model Platform (default physics/numerics)	Forcing	RMSE (m)
WvW3	NCEP	0.48
WvW3	NOGAPS+QuikSCAT (L2B, W6)	0.58
WAM4	NCEP	0.60
WvW3	NOGAPS	0.78
WAM4	NOGAPS	0.97

Table B16(a) — Error measures based on energy up to 0.06 Hz for January 2002 hindcast at location of NDBC buoy 46042 (west of Monterey, California). (WAM4 results were provided by Larry Hsu (NRL) and Paul Wittmann (FNMOC).)

January 2002. Buoy 46042. H_{m0} based on energy up to 0.06 Hz			
Model Platform (default physics/numerics)	Forcing	Bias (m)	RMSE (m)
WvW3	NOGAPS+QuikSCAT (L2B, W6)	–0.14	0.31
WAM4	NCEP	–0.14	0.33
WvW3	NCEP	–0.20	0.38
WAM4	NOGAPS	–0.44	0.59
WvW3	NOGAPS	–0.49	0.65

Table B16(b) — Same as Table B16(a), but for spectral energy up to 0.10 Hz

January 2002. Buoy 46042. H_{m0} based on energy up to 0.10 Hz		
Model Platform (default physics/numerics)	Forcing	Bias (m)
WvW3	NCEP	–0.03
WvW3	NOGAPS+QuikSCAT (L2B, W6)	0.03
WAM4	NCEP	–0.17
WvW3	NOGAPS	–0.47
WAM4	NOGAPS	–0.57
Model Platform (default physics/numerics)	Forcing	RMSE (m)
WvW3	NOGAPS+QuikSCAT (L2B, W6)	0.33
WvW3	NCEP	0.42
WAM4	NCEP	0.46
WvW3	NOGAPS	0.67
WAM4	NOGAPS	0.74